ELSEVIER

# Distribution of Dopamine $D_3$ Receptor Expressing Neurons in the Human Forebrain: Comparison with $D_2$ Receptor Expressing Neurons

*Eugenia V. Gurevich, Ph.D., and Jeffrey N. Joyce, Ph.D.*

*The dopamine $D_2$ and $D_3$ receptors are members of the $D_2$ subfamily that includes the $D_2$, $D_3$ and $D_4$ receptor. In the rat, the $D_3$ receptor exhibits a distribution restricted to mesolimbic regions with little overlap with the $D_2$ receptor. Receptor binding and nonisotopic in situ hybridization were used to study the distribution of the $D_3$ receptors and neurons positive for $D_3$ mRNA in comparison to the $D_2$ receptor/mRNA in subcortical regions of the human brain. $D_2$ binding sites were detected in all brain areas studied, with the highest concentration found in the striatum followed by the nucleus accumbens, external segment of the globus pallidus, substantia nigra and ventral tegmental area, medial preoptic area and tuberomammillary nucleus of the hypothalamus. In most areas the presence of $D_2$ receptor sites coincided with the presence of neurons positive for its mRNA. $D_3$ binding sites and $D_3$ mRNA positive neurons were most abundant in the limbic striatum and efferent structures, such as the nucleus accumbens, ventral striatum, substantia nigra, internal segment of the globus pallidus, anteroventral nucleus of the thalamus, and rostral pars reticulata of the substantia nigra. One important difference from the rat is that $D_3$ receptors were virtually absent in the ventral tegmental area. $D_3$ receptor and $D_3$ mRNA positive neurons were observed in sensory, hormonal, and association regions such as the nucleus basalis, anteroventral, mediodorsal, and geniculate nuclei of the thalamus, mammillary nuclei, the basolateral, basomedial, and cortical nuclei of the amygdala. As revealed by simultaneous labeling for $D_3$ and $D_2$ mRNA, $D_3$ mRNA was often expressed in $D_2$ mRNA positive neurons. Neurons that solely expressed $D_2$ mRNA were numerous and regionally widespread, whereas only occasional $D_3$-positive-$D_2$-negative cells were observed. The regions of relatively higher expression of the $D_3$ receptor and its mRNA appeared linked through functional circuits, but co-expression of $D_2$ and $D_3$ mRNA suggests a functional convergence in many regions of the signals mediated by the two receptor subtypes.*

***[Neuropsychopharmarmacology 20:60–80, 1999]***



KEY WORDS: *Dopamine $D_2$ receptor; Dopamine $D_3$ receptor; Receptor binding; Nonisotopic in situ hybridization; Human brain*

From the Christopher Center for Parkinson's Disease Research, Sun Health Research Institute, Sun City, AZ.

Address correspondence to: Eugenia V. Gurevich, Christopher Parkinson's Disease Research Center, Sun Health Research Institute, POB 1278, 10515 W Santa Fe Dr, Sun City, AZ 85372.

Received March 30, 1998; accepted July 16, 1998.

Dopaminergic transmission in the brain is believed to be involved in several neurological and psychiatric disorders such as schizophrenia, Parkinson's disease, and drug addiction. Five distinct subtypes of G-protein coupled dopamine (DA) receptors mediate the actions of DA, three of which, $D_2$, $D_3$, and $D_4$, belong to the $D_2$ family (Sibley et al. 1993). The $D_2$ receptor, the most highly expressed representative of this family, is thought to be the prime target of antipsychotic drugs



Published by Elsevier Science Inc.
655 Avenue of the Americas, New York, NY 10010

0893-133X/99/$–see front matter
PII S0893-133X(98)00066-9

used in the treatment of schizophrenia and thus has been studied extensively (for review see Joyce and Meador-Woodruff 1997). It is concentrated in major dopaminoceptive areas, primarily in the striatum, both in the rat and human brain (Bouthenet et al. 1987; Meador-Woodruff et al. 1991; Murray et al. 1994). Lower concentrations of $D_2$ binding sites and mRNA have also been observed in various extrastriatal brain regions suggesting that the $D_2$ receptor plays a role in their functions (Bouthenet et al. 1987; Janowski et al. 1992; Murray et al. 1994; Meador-Woodruff et al. 1994b, 1996).

In 1990 Sokoloff and associates (Sokoloff et al. 1990) cloned and characterized the rat DA $D_3$ receptor. It has high homology with the $D_2$ receptor and shares many pharmacological features of the latter including high affinity for $D_2$ receptor antagonists clinically used as antipsychotics. It has been proposed that the $D_3$ receptor is involved in schizophrenia pathology and antipsychotic action (Sokoloff et al. 1990; Gurevich et al. 1997; Joyce and Meador-Woodruff 1997), and plays a role in drug-seeking behavior (Caine and Koob 1993; Staley and Mash 1996). It has been shown that in the rodent the $D_3$ receptor is much less abundant than the $D_2$ receptor, has a restricted distribution, and exhibits a significant degree of segregation from the $D_2$ receptor in the nucleus accumbens (Bouthenet et al. 1991; Meador-Woodruff et al. 1991; Huang et al. 1992; Diaz et al. 1995; Le Moine and Bloch 1996). This limited distribution suggested a specific function for the D3 receptor subtype distinct from that of the D2 receptor and related to the mesolimbic rather than nigrostriatal system. In the human brain the $D_3$ receptor and its mRNA appear to be more widely distributed than in the rat (Landwehrmeyer et al. 1993; Meador-Woodruff et al. 1994a, 1994b, 1996; Murray et al. 1994; Suzuki et al. 1998), which may indicate a more extensive overlap of $D_3$ and $D_2$ receptors and more extensive role of the $D_3$ subtype in mediating actions of DA.

Most of our knowledge concerning localization of the $D_2$ and $D_3$ receptor subtypes in the human brain has been derived from experiments with in situ hybridization followed by low-resolution film autoradiography. Corresponding data on the distribution of $D_2$ and $D_3$ binding sites are often not available or have been obtained with non-selective radioligands. In this study we evaluated the distribution of $D_2$ and $D_3$ mRNA-positive neurons using non-isotopic in situ hybridization histochemistry (ISHH), which provides high cellular resolution. Systematic mapping of $D_2$ and $D_3$ receptor binding sites was used to compare the mRNA and receptor distributions. We also combined ISHH with immunochemistry to demonstrate the receptors' expression in the specific cell types and, for some regions, performed double-ISHH to detect their co-expression. This work extends previous studies of the $D_2$ and $D_3$ receptor distribution in the striatal and nigral areas and for the first time describes in detail the distribution of $D_2$ and $D_3$ binding sites and mRNAs in the basal forebrain, thalamic, hypothalamic, and amygdaloid nuclei. Our data support the hypothesis that in the human the D3 receptor is located, in addition to the limbic regions, in the sensory, motor, and association areas. The data were presented previously in their preliminary form (Gurevich and Joyce 1996).

## METHODS

### Subjects and Tissue Preparation

Frozen human brain tissue was obtained from the Hospital of the University of Pennsylvania (Dr. John Trojanowski, Director of Medical Pathology). Fixed cryoprotected sections of the human brain were obtained from the brain bank at Sun Health Research Institute. The left or right frozen hemispheres of 10 normal brains (5 males, 5 females) were used. Fixed sections from 6 normal cases (3 males, 3 females) were available from the left hemisphere only. The cases had no known history of neurological, neurovascular, or psychiatric disorder. Routine gross neuropathological and microscopic histopathological examination found no abnormalities in the tissue. The mean age at death was 68.7 $\pm$ 3.7 (frozen tissue) and 78.8 $\pm$ 1.5 (fixed tissue), mean post-mortem interval (PMI) was 13.2 $\pm$ 1.7 h (frozen tissue) and 1.8 $\pm$ 0.2 h (fixed tissue). Causes of death included respiratory failure, cardiac arrest, myocardial infarction, pneumonia, and various forms of cancer. No tissue from suicide victims was used in the study. All tissue used was acquired in 1994–95. Brain hemispheres were rapidly dissected into 1-cm thick slices, cut into slabs, and frozen in isopentane on dry ice. Fixed tissue was prepared by placing 1-cm thick slices dissected from left hemispheres in 4% paraformaldehyde in 0.1 M phosphate buffer for 48 h, placed in 2% dimethylsulfoxide, 10% glycerol in 0.1 M phosphate buffer for cryoprotection for 48 h, and then transferred to the same buffer with 20% glycerol. 40 μm-thick sections were cut on a freezing microtome, placed in 50% glycol, and stored at −20°C until needed. Two days before the experiment the sections were washed in phosphate buffered saline (PBS), treated with 3% $H_2O_2$/10% methanol in PBS to eliminate endogenous peroxidase activity, mounted on Vectabond (Vector Laboratories, Burlingame, CA) coated slides and air dried overnight. The next day the sections were defatted in chloroform:ethanol 1:1 overnight, rehydrated, and dried overnight before use in the experiments. Frozen sections (10–15 μm thick) were cut on Leica CM1900 cryostat and mounted on Probe-On Plus slides (Fisher, Pittsburgh, PA). The sections were fixed in 4% paraformaldehyde in PBS for 1 h at 4°C, washed 3 × 5 min in PBS, dehydrated in ethanols, dried, and stored at −80°C. Frozen sections were used for receptor

autoradiography and regular ISHH. Fixed sections were used for double ISHH and ISHH combined with immunohistochemistry.

### $D_2$ and $D_3$ Receptor Autoradiography

$D_2$ dopamine receptors were selectively labeled with [$^{125}$I]epidepride as described earlier (Murray et al. 1994). Dopamine $D_3$ receptors were labeled using selective agonist [$^{125}$I] 7-*trans*-hydroxy-PIPAT ([$^{125}$I] PIPAT) as described earlier (Gurevich et al. 1997). Dried sections were exposed to $^{3}$H-Hyperfilm for 18–72 h for [$^{125}$I] epidepride and 24–72 h for [$^{125}$I] PIPAT. Autoradiograms were developed using Kodak GBX developer (3 min) and fixer (5 min).

### In Situ Hybridization Histochemistry and Immunohistochemistry

***Probe Synthesis.*** The cDNA probe used to label the dopamine $D_2$ receptor was kindly provided by Dr. Roman Artymyshyn, University of Pennsylvania. The probe, 290 bp in length corresponding to the third cytosolic loop, recognized both long and short isoforms of the $D_2$ receptor. The full-size cDNA for the human $D_3$ receptor was a gift from Dr. Gurnam Gill, Pharmacia & UpJohn. Two probes for the $D_3$ receptor were constructed. One was 490 bp in length corresponding to IV and V transmembrane domains and part of the third cytosolic loop. The second probe was 447 bp in length and corresponded to the third cytosolic loop and VI membrane domain. Riboprobes were generated using $^{33}$P- (NEN, Boston, MA), digoxigenin-, or fluorescein-labeled UTP (Boehringer, Indianapolis, IN) in standard transcription reactions. Radioactive probes were phenol-chloroform purified and ethanol precipitated. Non-isotopic probes were prepared according to the manufacturer's instructions, and their concentrations were determined spectrophotometrically.

***Detection of $D_2$ and $D_3$ mRNA.*** Before hybridization the sections were treated with proteinase K (1 μg/ml) for 10 (frozen sections) or 30 (fixed sections) min at 37°C, incubated in 0.1 M triethanolamine with acetic anhydride for 15 min at room temperature, rinsed in 2 × SSC, dehydrated through ethanols and dried. Approximately 100 ng of digoxigenin or fluorescein-labeled or 2–5 × $10^6$ cpm of $^{33}$P-labeled probes in 60 μl of hybridization buffer containing 75% formamide, 50 mM Tris.HCl, 2.5 mM EDTA, 4 × SSC, 10% dextran sulfate, 1 mg/ml tRNA, 1 mg/ml calf thymus DNA was used for each section. The sections were incubated for 20 h at 55°C.

***Simultaneous Detection of $D_2$ and $D_3$ mRNAs.*** In double-labeling experiments the sections were hybridized with two probes, one fluorescein- and the other digoxigenin-labeled. Upon completion of hybridization the sections were rinsed in 4 × SSC to remove coverslips, washed in 50% formamide/2 × SSC for 15 min at 55°C, rinsed in 2 × SSC 2 × 10 min, treated with RNAse A (200 mg/ml) in 2 × SSC for 1 h at 37°C, washed in 2 × SSC 3 × 15 min, in 0.5 × SSC for 60 min at 55°C, in 0.1 × SSC for 60 min at 55°C, and in 0.1 × SSC for 10 min at room temperature. The sections were then incubated in a blocking solution containing 5% BSA and 0.3% Triton X-100 for 30 min at room temperature. Sheep anti-digoxigenin antibody (Fab fragment) conjugated with alkaline phosphatase was used at a 1:1000 dilution. Sheep anti-fluorescein peroxidase-conjugated antibody (Fab fragment) (Boehringer, Indianapolis, IN) was used at a dilution of 1:200. Fixed sections were treated with 0.3% $H_2O_2$ in methanol before use with peroxidase conjugated antibodies. In double-labeling experiments both antibodies were applied simultaneously. After incubation overnight at 4°C with the appropriate antibody, the sections were washed in PBS 3 × 10 min and in the appropriate substrate buffer for another 10 min at room temperature. The sections were then placed in substrate solution with incubation for 12–72 h at 37°C for alkaline phosphatase and at room temperature for peroxidase. 3,3′-Diaminobenzidine (DAB) (Sigma, St. Louis, MO) at a 0.05% concentration was used as a substrate for peroxidase. For alkaline phosphatase a mixture of nitroblue tetrasolium (0.34 mg/ml) and 5-bromo-4-chloro-3-indolyl phosphate (0.17 mg/ml) (NBT/BCIP) (Boehringer, Indianapolis, IN) was used. Substrate solutions contained 0.2 mg/ml of levamisol to block endogenous alkaline phosphatase activity. When the color developed, the sections were washed in 10 mM Tris/50 mM EDTA (TE) buffer for 30 min at room temperature, dehydrated in ethanol, washed in xylene, and mounted with Permount. In double-labeling experiments the sections were first incubated with DAB, washed in TE for 30 min, washed in the substrate buffer, and then incubated with NBT/BCIP substrate solution. When the color developed, the sections were again washed in TE buffer, dehydrated, and mounted from xylene with Permount. For sections containing the substantia nigra the double-labeling experiments were accomplished by using one $^{33}$P-labeled riboprobe and the one digoxigenin-labeled riboprobe. The non-isotopic probe was detected as described above, then sections were extensively washed in 1 × SSC, air dried, briefly dipped in 100% ethanol, dried, covered with 1% solution of cellulose nitrate in n-amyl acetate, dried, and dipped in nuclear emulsion (Ilford, Paramus, NJ). Emulsion-covered sections were exposed for 6–10 weeks at 4°C, developed at 17°C in D-19 Kodak developer for 3 min and fixed in 30% sodium thiosulfate for 5 min. The sections were then washed in water, allowed to air dry, and mounted with Permount.

***In Situ Hybridization Combined with Immunohistochemistry.*** When ISHH was followed by immunohistochemistry, the sections were blocked for 30 min at room temperature in PBS with 2% BSA and 0.3% Triton X-100, and incubated in PBS/1% BSA/0.3% Triton X-100 solution containing rabbit anti-choline acetyltransferase (ChAT) or anti-tyrosine hydroxylase (TH) (Chemicon, Temecula, CA) antibodies at a dilution of 1:500. The incubation was carried out overnight at 4°C. The ABC system (Vector Laboratories, Burlingame, CA) and AEC (Sigma, St. Louis, MO) or SG Blue (Vector Laboratories, Burlingame, CA) substrates for peroxidase were used for detection. Upon sufficient color development, the sections were washed in TE, rinsed in water, air dried overnight, and mounted with Permount. Sections containing the nucleus basalis (NBM or nucleus of the diagonal band (NDB) were hybridized with digoxigenin-labeled riboprobes for $D_2$ or $D_3$ receptors, as described above, then processed for ChAT immunohistochemistry. For sections containing the substantia nigra a $^{33}P$-labeled riboprobe was used. After standard post-hybridization washes, the sections were directly processed for TH immunohistochemistry. Following detection of antibody, the sections were washed in 1 × SSC, air dried overnight, and treated as described above.

***Controls.*** Respective sense riboprobes were used as a control for specificity of labeling. In double-labeling experiments control slides were also single-labeled for each mRNA species to determine the degree of changes introduced by the double-labeling procedure. With double-labeling protocols fewer cells were typically visible than with a single-labeling experiment. The reverse order of incubation in the substrate solutions (NBT/BCIP first and DAB second) was tested to optimize the visualization conditions. Though the protocol finally adopted (fluorescein-labeled $D_3$ probe visualized first with DAB followed by digoxigenin-labeled $D_2$ probe) appeared to be superior in visual identification of double-labeled cells, the reverse order produced the same general pattern of labeling. In the experiments with ISHH followed by immunohistochemistry control slides were also run for single detection of ISHH and immunodetection, as well as control slides with primary antibody substituted with non-immune serum. We found that if immunochemical labeling was preceded by ISHH a proportion of antigenic sites appeared to be lost, which may be due to proteinase treatment employed in the ISHH protocol. The reverse order (immunochemistry first and ISHH second) usually resulted in a certain degradation of the hybridization signal and required care to ensure RNAse-free conditions during the immunohistochemical procedure. The protocol finally adopted appeared to be superior in preserving both hybridization and immunochemical signals.

### Microscopy, Anatomy, and Data Analysis

Autoradiograms of the binding to $D_2$ and $D_3$ binding sites were analyzed using Macintosh-based imaging system and Brain for Macintosh software, version 2.0 (Drexel University, Philadelphia, PA). $^3H$ plastic standards calibrated for $^{125}I$ were used to convert gray values into fmol/mg of bound ligands. Sections processed for ISHH were examined and photographed using Nikon Optiphot microscope. Density of labeled cells was determined by visual examination and assessed as high, moderate, low, occasional cells detected, and not detected. These ratings do not take into account differences in the staining intensity. Adjacent sections stained for $D_2$ or $D_3$ mRNA were analyzed simultaneously, and the criteria used to assign the ratings were the same for both mRNA species. A number of technical considerations makes quantitative comparison of different mRNAs' levels problematic. However, semi-quantitative comparison should provide sufficient initial estimate of the distribution and comparative frequency of $D_2$ and $D_3$ mRNA expressing neurons in the human brain. Quantitation of cells double-labeled for $D_2$ and $D_3$ mRNA was done using C-Imaging Image analysis system (Compix Inc, Cranberry Township, PA) equipped with DAGE MTI-81 high resolution color videocamera. Images were collected in RGB mode, and double- and single-labeled cells were identified based on intensity levels of red, green, and blue components. Number of double-labeled, total number of labeled cells, and respective areas they occupy in each viewfield were measured. Seven to 10 viewfield per case and 3–4 cases per brain area were analyzed. Proportions of double-labeled cells to all labeled cells were calculated for each brain area examined. Values were averaged for each case, and means were determined across cases.

Adjacent sections were stained for Nissl and AChE to identify structures. A number of references were used to aid in the identification of the structures examined (Haber and Groenewegen 1989; Jones 1990; Sims and Williams 1990; Heckers et al. 1992). The basal ganglia structures were identified as described by Alheid et al. (1990). The thalamic nuclei were delineated and named according to Ohye (1990) and Armstrong (1990). The hypothalamic nuclei were delineated and named according to Saper (1990). Identification and nomenclature of the amygdaloid nuclei were based primarily on the work of de Olmos (1990). The dopaminergic cell groups in the midbrain were identified and described based on nomenclature given by Paxinos et al. (1990).

## RESULTS

We surveyed the distribution of $D_2$ and $D_3$ receptor binding sites and $D_2$ and $D_3$ mRNA positive neurons in

the subcortical areas of the human brain including the caudate (CN), putamen (Pu), nucleus accumbens (NAC), globus pallidus (GP), ventral pallidum (VP), basal forebrain, thalamus, hypothalamus, amygdala, and substantia nigra (SN). Abbreviations used throughout the text are provided in Table 1. Binding densities for $D_2$ and $D_3$ receptors and assessments of frequency of neurons positive for respective mRNA are summarized in Table 2.

**Table 1.** Abbreviations

ac, anterior commissure;
AHA, anterior hypothalamic area;
AM, anteromedial nucleus of the thalamus;
APir, amygdalopiriform transitional area;
AStr, amygdalostriatal transitional area;
AV, anteroventral nucleus of the thalamus;
BL, basolateral nucleus of the amygdala;
BM, basomedial (accessory) nucleus of the amygdala;
Ce, central nucleus of the amygdala;
CeM, central medial nucleus of the thalamus;
CeL; central lateral nucleus of the thalamus;
CL, claustrum;
CLi, caudal linear raphe nucleus;
CN, caudate nucleus;
Co, cortical nucleus of the amygdala;
CPu, caudate putamen;
Crb, cerebellum;
Ctx, cortex;
$D_2$, dopamine $D_2$ receptor subtype;
$D_3$, dopamine $D_3$ receptor subtype;
DHA, dorsal hypothalamic area;
DL, dorsolateral subdivision of the basolateral nucleus of the amygdala;
D, dorsal subdivision of the basolateral nucleus of the amygdala;
fx, fornix;
GPe, external segment of the globus pallidus;
GPi, internal segment of the globus pallidus;
I, intermediate subdivision of the basolateral nucleus of the amygdala;
ic, internal capsula;
ICj, islands of Calleja;
La, lateral nucleus of the amygdala;
LD, laterodorsal nucleus of the thalamus;
LGN, lateral geniculate nucleus;
LHA, lateral hypothalamis area;
LM, lateral mammillary nucleus;
LP, nucleus lateralis posterior of the thalamus;
Me, medial nucleus of the amygdala;
MD, mediodorsal nucleus of the thalamus;
mf, mammillary fasciculus;
MGN, medial geniculate nucleus;
MM, mammillary bodies;
mtt, mammillothalamic tract;
NAC, nucleus accumbens;
NDB, nucleus of the diagonal band of Broca;
NBM, nucleus basalis of Meynert;
NR, nucleus reuniens of the thalamus;
ot, optic tract;

(*continued*)

**Table 1.** (*continued*)

P, pulvinar nucleus of the thalamus;
PBP, parabrachial pigmented nucleus;
Pc, paracentral nucleus of the thalamus;
PHA, posterior hypothalamis area;
PL, paralaminar subdivision of the basolateral nucleus of the amygdala;
PN, paranigral nucleus;
Pu, putamen;
RLi, rostral raphe nucleus;
SG, suprageniculate nucleus;
SN, substantia nigra;
SNc, substantia nigra pars compacta;
SN1, substantia nigra pars lateralis;
SNr, substantia nigra pars reticulata;
STh, subthalamic nucleus;
VA, nucleus ventralis anterior;
VL, ventrolateral subdivision of the basolateral nucleus of the amygdala;
VLa, nucleus ventralis lateralis anterior of the thalamus;
VLp, nucleus ventralis lateralis posterior of the thalamus;
Vm, ventromedial subdivision of the basolateral nucleus of the amygdala;
VP, ventral pallidum;
VPL, nucleus ventralis lateralis posterior of the thalamus;
VTA, ventral tegmental area;
ZI, zona inserta.

## Basal Ganglia and Basal Forebrain

In agreement with data reported earlier (Joyce et al. 1986; Murray et al. 1994), the concentration of $D_2$ receptors was found to be highest in the rostral CN and Pu, with the sites distributed evenly through the dorsoventral extent of the striatum (Table 2 and Figure 1A). In contrast, $D_3$ receptors were more abundant in the NAC and ventral aspect of the rostral Pu and were concentrated in areas of dense binding giving both structures a patchy appearance (Table 2 and Figure 1B) as reported previously (Murray et al. 1994; Gurevich et al. 1997). Striatal concentrations of both $D_2$ and $D_3$ receptor sites tended to decline along the rostro-caudal axis of the striatum. Both $D_2$ and $D_3$ receptor sites were also present in the GP (Figure 1). The concentration of $D_2$ receptors was considerably higher in the external (GPe) as opposed to the internal segment of the GP (GPi), whereas $D_3$ receptor concentrations were comparable in both segments. In the GPi $D_3$ sites were more abundant than $D_2$ sites, accounting for more than 70% of combined $D_2$ and $D_3$ binding site concentration, especially at the rostral level (Table 2, Figure 1, and Figure 2B). The concentration of $D_3$ sites was also high in the rostral VP (Figure 2A).

$D_2$ receptor mRNA was expressed in many neurons in the Pu, CN, and the NAC (Figure 3A and 4A). The neurons expressing $D_2$ mRNA appeared to be distributed evenly over the striatum. $D_3$ mRNA positive neurons were also found throughout the striatum (Figure

**Table 2.** Concentrations of $D_2$ and $D_3$ binding sites[a] and densities of $D_2$ and $D_3$ receptor mRNA expressing neurons[b] in the subcortical areas of the human brain

| Regions | $D_2$ receptor binding, fmol/mg | $D_3$ receptor binding, fmol/mg | $D_2$ mRNA | $D_3$ mRNA |
|---|---|---|---|---|
| Basal ganglia and basal forebrain | | | | |
| Dorsal caudate nucleus | 64.2 ± 4.5 | 9.65 ± 1.36 | +++ | +++ |
| Ventral caudate nucleus | 55.8 ± 4.5 | 13.84 ± 2.04 | +++ | +++ |
| Dorsal putamen | 67.9 ± 5.5 | 15.60 ± 2.72 | +++ | +++ |
| Ventral putamen | 63.9 ± 5.2 | 22.17 ± 3.3 | +++ | +++ |
| Nucleus accumbens | 49.3 ± 7.8 | 24.8 ± 3.9 | +++ | +++ |
| Tail of caudate | 48.7 ± 6.1 | 7.67 ± 1.09 | +++ | ++ |
| Globus pallidus external | 15.5 ± 2.8 | 7.37 ± 1.31 | ++ | ++ |
| Globus pallidus internal | 2.32 ± 0.55 | 9.34 ± 1.34 | ++ | ++ |
| Ventral pallidum | 7.35 ± 2.69 | 10.6 ± 3.22 | ++ | ++ |
| Nucleus basalis | 17.5 ± 12.46 | 3.84 ± 1.3 | ++ | ++ |
| Thalamus | | | | |
| Anteroventral nucleus | 3.21 ± 0.44 | 4.96 ± 0.46 | ++ | ++ |
| Mediodorsal nucleus | 3.0 ± 1.23 | 1.53 ± 0.43 | ++ | ++ |
| Ventral anterior nucleus | 2.39 ± 0.4 | 2.16 ± 1.24 | ++ | +/− |
| Ventral lateral anterior nucleus | 3.05 ± 1.45 | 0.98 ± 0.5 | + | +/− |
| Ventral lateral posterior nucleus | 2.62 ± 1.29 | 1.37 ± 0.45 | + | +/− |
| Central medial nucleus | 5.42 ± 1.15 | n/d | + | n/d |
| Central lateral nucleus | 3.69 ± 0.92 | n/d | + | n/d |
| Reuniens nucleus | 3.19 ± 0.33 | 2.92 ± 1.4 | + | + |
| Paracentral nucleus | 2.63 ± 0.53 | n/d | + | n/d |
| Ventral posterior lateral nucleus | 0.98 ± 0.14 | n/d | + | +/− |
| Lateral geniculate nucleus | 1.54 ± 0.08 | 0.86 ± 0.27 | ++ | ++ |
| Medial geniculate nucleus | 1.93 ± 0.37 | 0.8 ± 0.29 | + | + |
| Mammillothalamic tract | n/d | 5.79 ± 0.38 | n/d | +/− |
| Subthalamic nucleus | 4.17 ± 0.69 | n/d | ++ | n/d |
| Hypothalamus | | | | |
| Medial preoptic area | 8.45 ± 1.55 | n/d | ++ | + |
| Dorsal hypothalamic area | 5.37 ± 0.76 | n/d | ++ | + |
| Anterior hypothalamic area | 4.84 ± 1.9 | n/d | ++ | + |
| Paraventricular nucleus | 5.49 ± 1.55 | 1.04 ± 0.19 | ++ | +/− |
| Dorsomedial nucleus | 3.83 ± 1.58 | n/d | ++ | +/− |
| Ventromedial nucleus | 2.82 ± 0.45 | n/d | ++ | +/− |
| Lateral hypothalamic area | 4.56 ± 1.16 | 1.72 ± 0.39 | ++ | + |
| Arcuate nucleus | 8.53 ± 1.28 | n/d | ++ | +/− |
| Posterior hypothalamic area | 5.49 ±1.55 | 1.84 ± 0.19 | ++ | + |
| Tuberomammillary nucleus | 7.86 ± 1.38 | 2.18 ± 0.68 | ++ | +/− |
| Supramammillary nucleus | 5.66 ± 1.1 | 1.87 ± 0.28 | ++ | +/− |
| Mammillary nuclei | 2.34 ± 0.73 | 4.32 ± 1.47 | + | ++ |
| Mammillary fasciculus | n/d | 5.79 ± 0.38 | n/d | +/− |
| Amygdala | | | | |
| Amygdalostriatal transitional area | 10.98 ± 1.97 | 2.4 ± 0.03 | ++ | + |
| Amygdalopiriform transitional area | n/d | 1.7 ± 0.51 | + | + |
| Central nucleus | 2.64 ± 0.89 | 1.56 ± 0.28 | + | − |
| Cortical nucleus | n/d | 1.65 ± 0.4 | + | + |
| Basolateral nucleus dorsolateral division | 5.03 ± 2.2 | 2.48 ± 0.4 | ++ | + |
| Basolateral nucleus dorsal division | 5.69 ± 2.32 | 2.54 ± 0.46 | ++ | + |
| Basolateral nucleus intermediate division | 5.91 ± 3.0 | 2.35 ± 0.3 | ++ | +/− |
| Basolateral nucleus paralaminar division | 4.04 ± 3.1 | 1.9 ± 0.14 | + | +/− |
| Basolateral nucleus ventromedial division | 5.75 ± 3.5 | 1.77 ± 0.17 | + | +/− |
| Basolateral nucleus ventrolateral division | 3.64 ± 2.33 | 1.9 ± 0.25 | + | +/− |
| Basomedial (accessory) nucleus | n/d | 1.85 ± 0.22 | + | + |
| Lateral nucleus | 1.35 ± 0.45 | 0.96 ± 0.37 | + | + |
| Substantia nigra and ventral tegmental area | | | | |
| Substantia nigra pars compacta | 15.44 ± 3.56 | 5.07 ± 0.64 | ++ | ++ |
| Substantia nigra pars reticulata | 9.78 ± 1.54 | 4.19 ± 0.18 | ++ | ++ |

(*continued*)

**Table 2.** (*continued*)

| Regions | $D_2$ receptor binding, fmol/mg | $D_3$ receptor binding, fmol/mg | $D_2$ mRNA | $D_3$ mRNA |
|---|---|---|---|---|
| Substantia nigra pars reticulata rostral | 3.44 ± 0.52 | 11.33 ± 1.78 | ++ | ++ |
| Substantia nigra pars lateralis | 12.07 ± 2.73 | 3.1 ± 0.4 | ++ | ++ |
| Paranigral nucleus | 13.18 ± 2.83 | n/d | + | +/− |
| Parabrachial pigmented nucleus | 10.58 ± 1.93 | n/d | + | +/− |
| Caudal linear raphe nucleus | 7.69 ± 1.00 | n/d | + | n/d |

[a] Autoradiographic experiments with [$^{125}$I] epidepride and [$^{125}$I]PIPAT were carried out using concentrations of the radioligands equal their respective $K_d$s. This makes concentrations of $D_2$ and $D_3$ binding sites roughly comparable, even though Bmax values were not obtained. We have previously studied binding of both radioligands in various brain areas and found no significant differences in $K_d$s[13, 40] that supports validity of comparing binding site concentrations in various area measured at single concentration of a radioligand. n/d - specific binding not detected.

[b] Density of cells stained for $D_2$ or $D_3$ receptor mRNA were assessed as +++-high, ++-moderate, +-low, +/−- occasional cells observed, n/d- not detected. The same criteria were used to assess frequencies of cells stained for $D_2$ and $D_3$ mRNA.

3B and 4B), though their frequency was lower than that of $D_2$ mRNA positive neurons. $D_3$ mRNA positive cells were relatively abundant in the NAC and ventral portion of the Pu and less abundant in the CN and dorsal PU (data not shown). However, even in the NAC a considerable proportion of neurons appeared to be negative for $D_3$ mRNA (Figure 4B). $D_2$ mRNA was easily detectable in medium spiny striatal neurons as well as in large, presumably cholinergic, interneurons (Figure 3A, arrow, and 3D), whereas only very few large neurons in CN and Pu were stained for $D_3$ mRNA, and most labeled cells were medium in size (Figures 3B and 3F). $D_3$

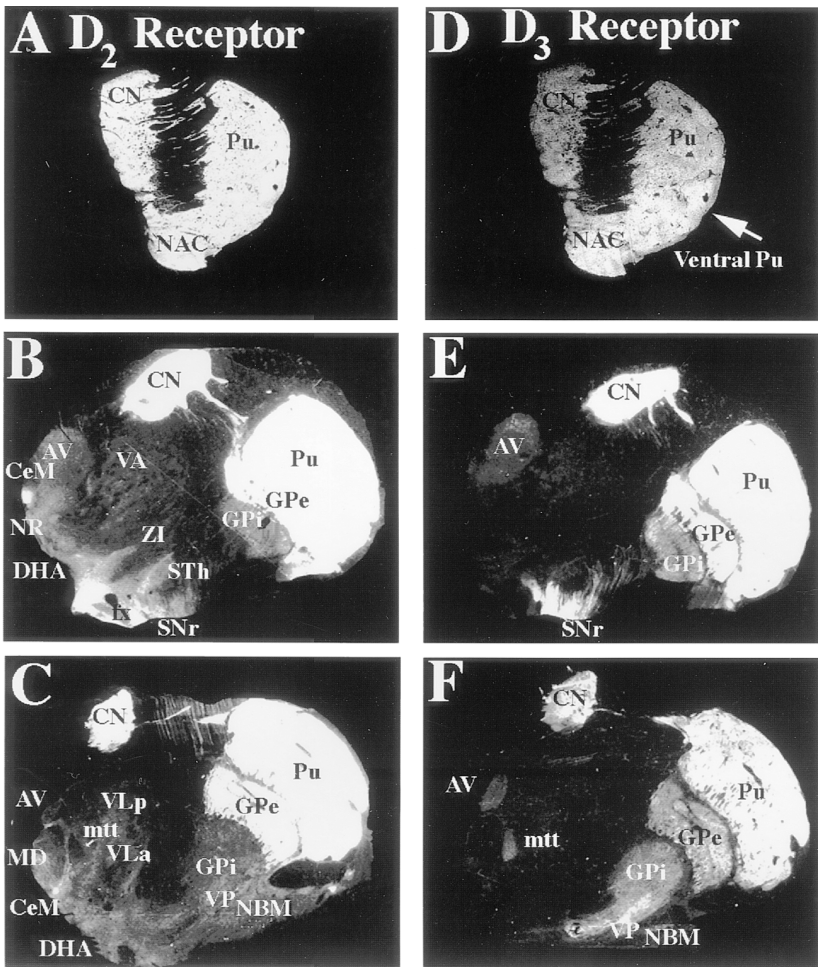


**Figure 1.** Darkfield photomicrographs of [$^{125}$I]epidepride binding to $D_2$ and $D_3$ receptors in the rostral striatum (A, D) and two rostro-caudal levels of the basal ganglia, thalamus, and hypothalamus (B, E and C, F). Adjacent sections were labeled with 50 pM [$^{125}$I]epidepride in the presence of 100 μM Gpp and either 100 nM 7-OH-DPAT (to block $D_3$ receptors) to visualize $D_2$ receptors (left panel) or 10 μM domperidone (to block $D_2$ receptors) to visualize $D_3$ receptors (right panel). Photographs represent specific binding. There is an evident gradient of $D_3$ receptors in the rostral striatum (B) with the highest binding in the NAC and ventral Pu not evident for $D_2$ receptors (A). Arrow in B indicates the border of increased $D_3$ binding in the ventral Pu. Autoradiograms in B, C, E, and F were deliberately overexposed to allow for visualization of binding to $D_2$ and $D_3$ receptors in extrastriatal areas. Note the relatively high concentrations of $D_3$ receptors in the GPi and SNr compared to $D_2$ receptors, labeling of the intralaminar thalamic nuclei for $D_2$ but not $D_3$, and much higher concentrations of $D_2$ than $D_3$ sites in the hypothalamus. Also note the presence of $D_3$ receptors and the absence of $D_2$ receptors in mtt. All abbreviations are as in Table 1.

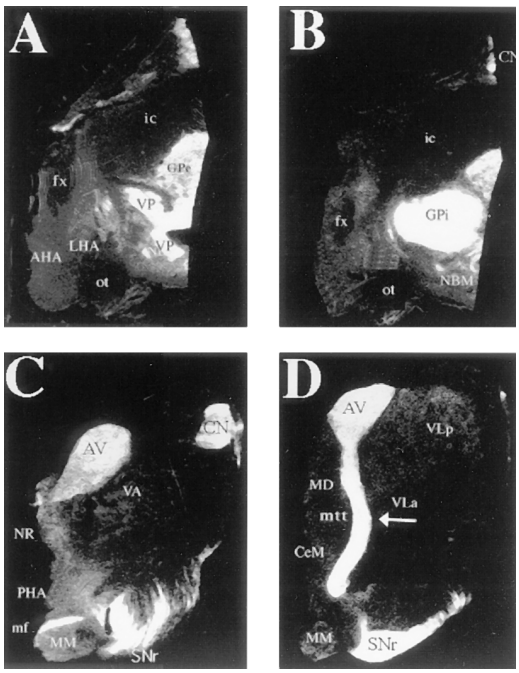


**Figure 2.** Darkfield photomicrographs of [$^{125}$I]7-*trans*-hydroxy-PIPAT to $D_3$ receptors. Coronal sections at four rostro-caudal levels (A, B, C, D) containing the striatum, thalamus, and hypothalamus are shown. Note high concentrations of $D_3$ sites in the VP (A), Gpi (B), and SNr (C, D) and the labeling of the AV and mtt in the thalamus (C, D). D, arrow indicates the border where elevated concentration of $D_3$ sites coincides with the presence of $D_3$ mRNA positive cells within the mtt. Also note the presence of very low concentration of $D_3$ sites throughout the thalamus and hypothalamus. All abbreviations are as in Table 1.

mRNA expressing neurons in the NAC tended to appear in clusters, whereas $D_2$ positive neurons were distributed more evenly. $D_2$ and $D_3$ mRNA expressing cells were detected in both the GPe and GPi (Figures 3G and 3H). In the GPe the frequency of the $D_3$ mRNA-expressing neurons was lower than that of $D_2$ mRNA-expressing neurons, whereas in the GPi frequency of each type of labeled cells appeared to be similar (Figures 3G and 3H). $D_3$ mRNA positive neurons were frequently found clustered at the medial pole of the internal segment, the area that also displayed a high concentration of $D_3$ receptor sites (Figures 1F and 2B). Some neurons in the globus pallidus co-expressed $D_2$ and $D_3$ mRNA, but many appeared to be labeled only for one or the other mRNA species, most often for $D_2$ mRNA (Figures 4E).

In the magnocellular complex of the basal forebrain the concentration of $D_2$ receptor sites was higher than that of $D_3$ sites (Table 2; Figures 1C and 1D, and 2A, B). $D_2$ and $D_3$ mRNAs were found in both vertical and horizontal subdivisions of the NDB as well as in NBM. Staining density of most cells and frequency of stained neurons appeared to be higher for $D_2$ than $D_3$ mRNA. ISHH combined with immunohistochemistry demonstrated that neurons positive for ChAT were often positive for $D_2$ and $D_3$ mRNAs (Figures 4C and D). Double-labeling experiments demonstrated that $D_2$ and $D_3$ mRNAs were co-expressed in 38.2 ± 6.0% of labeled neurons in both nuclei (Figure 4F).

### Thalamus and Hypothalamus

In the human thalamus we found differing patterns for the distribution of $D_2$ and $D_3$ binding sites. Moderate to low concentrations of $D_2$ sites were found in all thalamic nuclei (Table 1; Figures 1A and C). The highest $D_2$ receptor concentration was found in the intralaminar nuclei, especially in the central medial nucleus (Figures 1A and C; Figure 5B; arrows). The anterior thalamus had a slightly higher $D_2$ receptor concentration than most other nuclei. In the posterior thalamus the geniculate nuclei, both medial (MGN) and lateral (LGN) and ventral posterolateral nucleus possessed $D_2$ sites in low concentrations (Figure 5B). As exemplified in Figures 1B and D, $D_3$ receptors were also relatively abundant in the AV. Other nuclei in the rostral thalamus displayed measurable but low $D_3$ binding. Interestingly, $D_3$ binding sites were also found in the mammillo-thalamic tract (mtt), starting at its point of origin in the mammillary nuclei (MM) (Figure 2C) and ascending throughout the length of the tract to the AV (Figures 1D and 2D). The concentration of $D_3$ receptor sites in the tract, especially in its ventral portion, was equal to or higher than in the target structure or in the MM. With the aid of adjacent sections stained for Nissl and AChE, we took special care to distinguish between the mtt and the intralaminar nuclei, which are embedded in the internal medullary lamina of the thalamus, and confirmed that $D_3$ binding sites were indeed located in mtt itself. The origin of $D_3$ binding sites in mtt is not clear. However, the same organization of $D_3$ receptors in the mtt and attendant nuclei was observed in the rat brain, where $D_3$ receptors were present in the anterior nuclei (anterodorsal and anteromedial) of the thalamus and MM as well as in the mtt (Figure 6). In contrast, $D_2$ receptors were not found in the mtt, though present in all intralaminar nuclei contained within the internal medullary lamina of the thalamus. This suggests an important role for the $D_3$ receptor in regulating afferents to the anterior nuclei of the thalamus that is conserved across species. In the posterior part of the thalamus modest $D_3$ binding was observed in the geniculate bodies, especially in the LGN (Figure 5C).

Localization of $D_2$ and $D_3$ receptor mRNA expressing cells in the human thalamus generally, but not always, matched that of the respective receptor sites. Numerous $D_3$ as well as $D_2$ positive neurons were observed in the AV (Figure 7E). The MD was also comparatively rich in

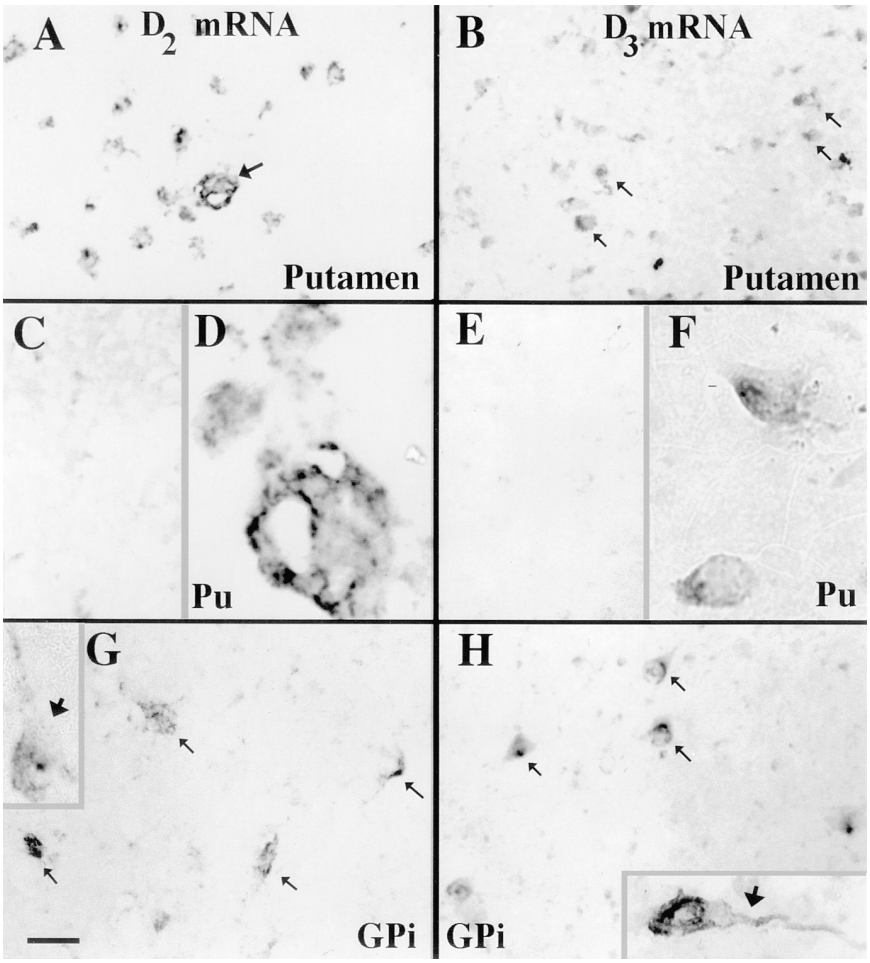


**Figure 3.** Neurons labeled for $D_2$ (left panel) and $D_3$ receptor (right panel) mRNA in the Pu and globus pallidus. A and B, Pu; C and E, Pu, labeling with corresponding sense probes; D and F, Pu, enlarged to show details; G and H, GPi (inserts: enlarged individual pallidal neurons labeled for $D_2$ and $D_3$ mRNA, respectively). Arrow in A indicates large presumably cholinergic interneuron labeled for $D_2$ mRNA (the same large cell is shown in D). Arrows in B, G, and H indicate some of the cells labeled for respective mRNA. Large arrows in inserts in G and H show the presence of mRNA in the processes of the pallidal neurons. Bar = 40 μm (10μm in D and F; 23 μm in inserts in G and H).

$D_2$ and $D_3$ mRNA expressing cells (Figure 7C). $D_3$ positive neurons tended to be concentrated along the midline, while $D_2$ positive cells were more homogeneously distributed across the medio-lateral extent of the nucleus. The intralaminar thalamic nuclei had both high numbers of $D_2$ receptors (Figure 5B) and a considerable number of $D_2$ mRNA positive neurons (Figure 7D). $D_3$ receptor sites in the mtt did not appear to match the location of $D_3$ mRNA positive neurons. Neurons could be seen on Nissl and AChE preparations embedded in the tract. A number of $D_3$ mRNA positive neurons could also be observed within the tract. In Figure 2D, an arrow indicates the border of increased $D_3$ binding coincident with an expansion in the number of $D_3$ mRNA positive cells within the tract. However, these cells within the tract were by no means more numerous or darker stained than cells in adjacent areas. $D_2$ mRNA positive cells were also observed invading the tract, though $D_2$ receptor sites were not detected there. Some $D_3$ mRNA positive cells were visible in the lower portion of the tract, but not in sufficient quantity to account for the high concentration of $D_3$ receptor sites in this area. $D_3$ receptors may also be synthesized by neurons of the neighboring nuclei that enter the tract to meet the fibers. Alternatively, the receptor sites may be located on the collaterals of the mammillary fibers forming the tract. The MM neurons are rich in $D_3$ mRNA with only moderate concentration of $D_3$ sites. Thus, the receptors may be transported to the processes of the mammillary neurons.

Among other thalamic nuclei, relatively numerous neurons expressing $D_2$ mRNA and occasional neurons expressing $D_3$ mRNA were found in the ventral anterior, lateral dorsal, ventral posteromedial, parafascicular, posterior, and pulvinar nuclei, where concentrations of both $D_2$ and $D_3$ sites were low. Large neurons at the lateral border of the ventral posterolateral nucleus, in the area where $D_2$ receptor sites were present (Figure 5B), stained intensely for $D_2$ mRNA (Figure 7F). $D_3$ mRNA positive neurons were also observed in this area despite a virtual absence of $D_3$ receptor sites. The LGN displayed a high occurrence of $D_2$ (data not shown) and $D_3$ (Figure 7A) mRNA positive neurons, which is consistent with the presence of both $D_2$ and $D_3$ receptor sites (Figures 5B and C). The MGN had concentrations of $D_2$ and $D_3$ receptors comparable to the LGN but a much lower frequency of $D_2$ (Figure 7B) or $D_3$ mRNA positive neurons.

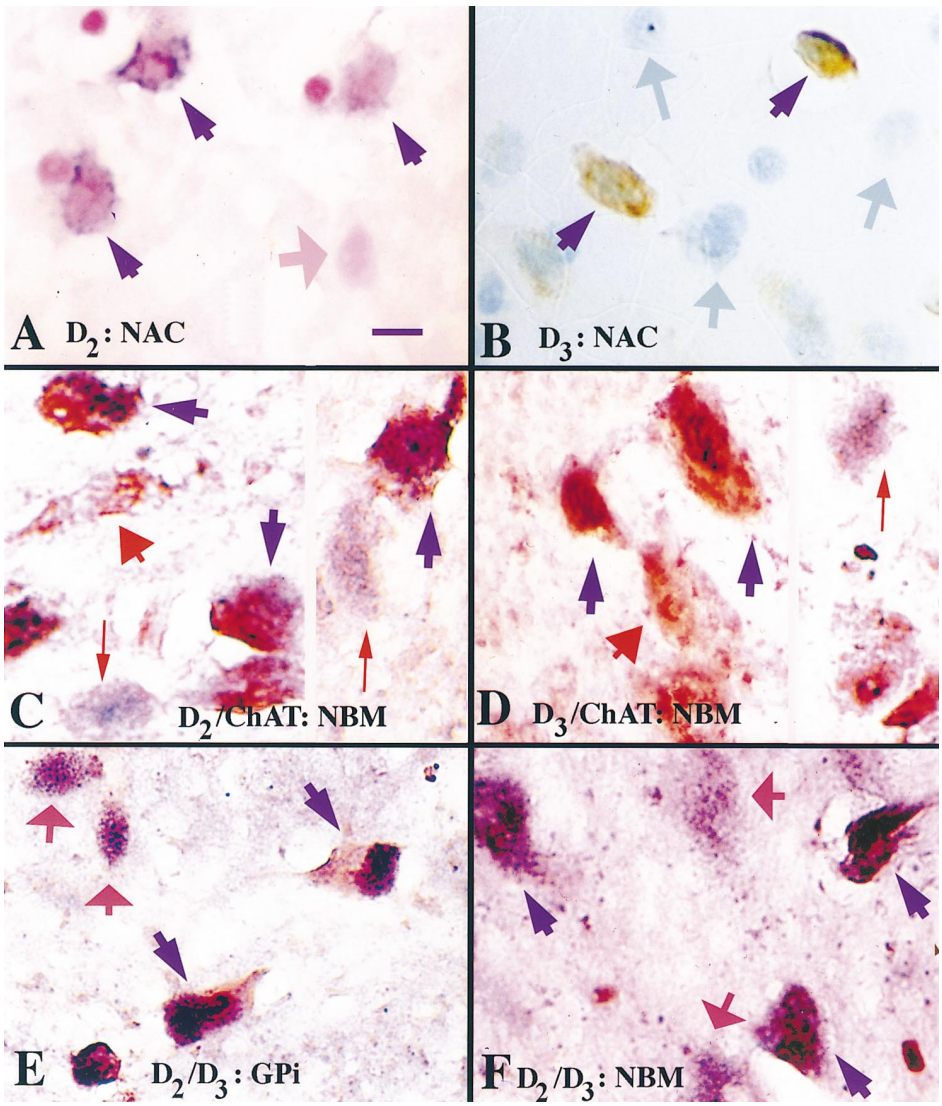


**Figure 4.** $D_2$ and $D_3$ mRNA positive neurons in the basal ganglia and basal forebrain. A and B, sections of the NAC labeled for $D_2$ mRNA with the digoxigenin-labeled riboprobe (A) and $D_3$ mRNA with the fluorescein-labeled riboprobe (B) and counterstained with Nuclear Fast Red (A) or Methyl Green (B). Purple arrows indicate respective mRNA positive neurons; pink or blue arrows = mRNA negative neurons. C and D, co-localization of $D_2$ (C) and $D_3$ (D) mRNA with ChAT immunoreactivity in the NBM. $D_2$ and $D_3$ mRNAs were visualized as purple precipitate with distinct granular appearance. ChAT immunoreactivity was visualized as bright red color. Double-labeled cells have both colors overlapped or partially separated. Purple arrows indicate double-labeled cells; large red arrows = ChAT positive cells; small red arrows = $D_2$ or $D_3$ positive cells. Right and left panel photographs in C and D were taken from different sections. E and F, double-staining for $D_2$ and $D_3$ mRNA in the GPi (E) and NBM (F). D2 mRNA was visualized as purple granulated precipitate and $D_3$ mRNA as brown more homogeneously looking precipitate. Purple arrows indicate double-labeled neurons; red arrows = $D_2$ mRNA positive neurons. Bar in A and B = 8.7 μm, in C–F = 17 μm.

Generally $D_3$ mRNA-expressing neurons tended to concentrate along the midline of the thalamus, and the staining intensity was higher in the neurons close to midline than in the more laterally located cells. $D_2$ receptor mRNA-expressing neurons were distributed more uniformly throughout the thalamus, and their density was higher than that of $D_3$ mRNA-expressing neurons. Double labeling for $D_2$ and $D_3$ mRNA revealed the presence of neurons that expressed both mRNA species throughout the thalamus. They were more numerous along the midline, particularly in the AV and MD (Figures 8C and D), where $D_3$ expressing neurons were more likely to be found. In the more lateral parts of the thalamus the majority of neurons solely stained for $D_2$ mRNA. Double-labeled neurons accounted for 31.6 ± 5.3 and 20.9 ± 1.0% of labeled cells in AV and MD, respectively, as opposed to 11.7 ± 0.7% in the ventral anterior nucleus. $D_3$ mRNA could be detected in large

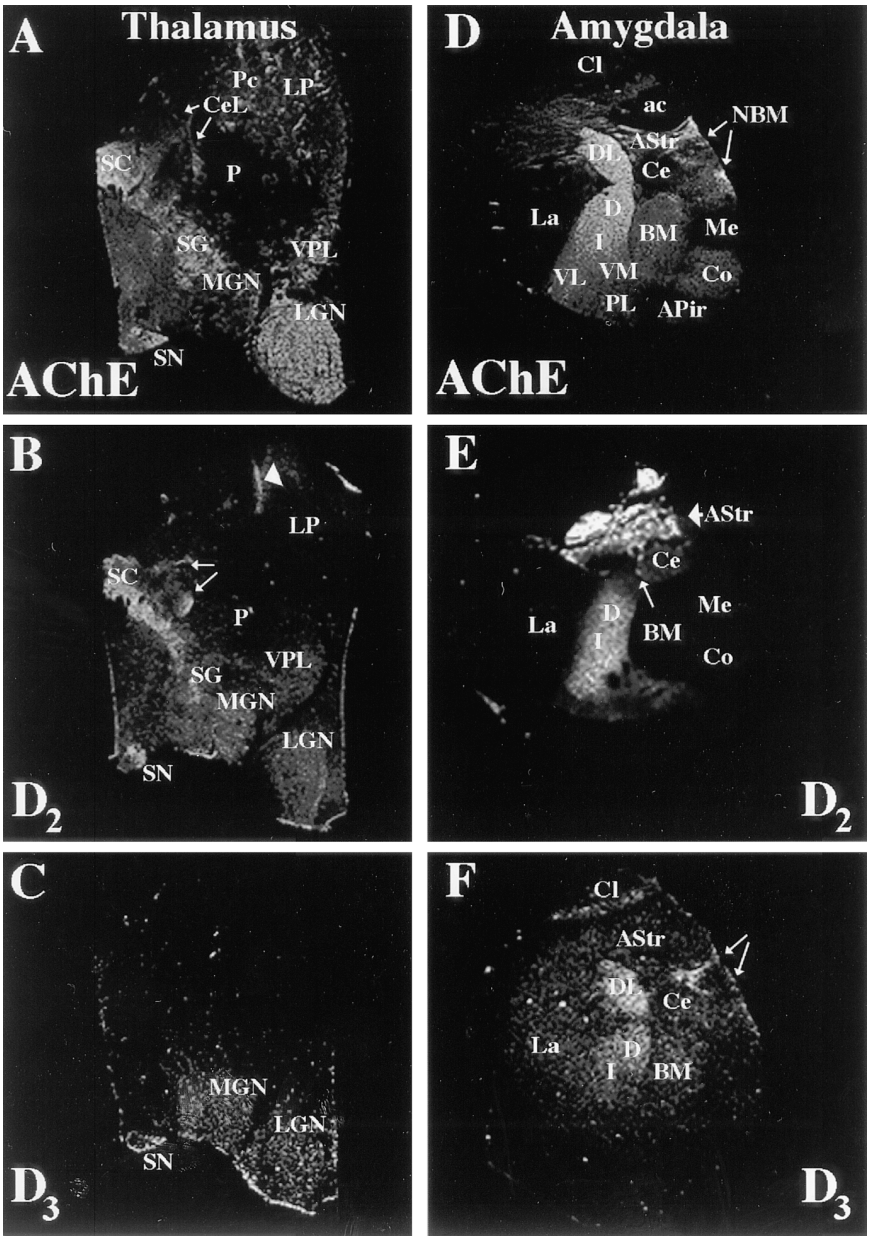


**Figure 5.** Sections of the thalamus (A–C) and amygdala (D–F) stained for AChE (A, D), and labeled for $D_2$ receptors (B, E) with [$^{125}$I]epidepride (in the presence of 7-OH-DPAT to block $D_3$ receptors) or for $D_3$ receptors (C, F) with [$^{125}$I]PIPAT (all photographs represent specific binding). Arrows in B indicate the binding corresponding to the central lateral nucleus of the thalamus; arrowhead = to paracentral nucleus of the thalamus; arrow in E shows the areas of high $D_2$ binding in the lateral part of the central nucleus of amygdala that corresponds to the location of cells intensely labeled for $D_2$ mRNA demonstrated in Figure 9 B; arrows in F indicate the area of binding corresponding to the NBM. Also note relatively high levels of $D_3$ receptors in the dorsolateral and dorsal subdivision of the BL in the amygdala. All abbreviations are as in Table 1.

neurons, most of which also expressed $D_2$ mRNA, in the lateral part of the ventral posterolateral nucleus (Figure 8A). A considerable number of double-labeled neurons were observed in the LGN, especially large neurons within the first layer (Table 2). In the upper layers of the LGN $D_2$ mRNA positive neurons were more frequent than double-labeled neurons (Table 2 and Figure 8F). In the layer I of LGN double-labeled neurons represented 48.3 ± 6.5% of all labeled cells, whereas in the upper layer only 22.0 ± 3.8% of cells were double-labeled. Neurons selectively labeled for $D_3$ mRNA were encountered, albeit rarely (Figure 8E).

In the hypothalamus $D_2$ receptor sites were observed in all major areas without substantial variation in the

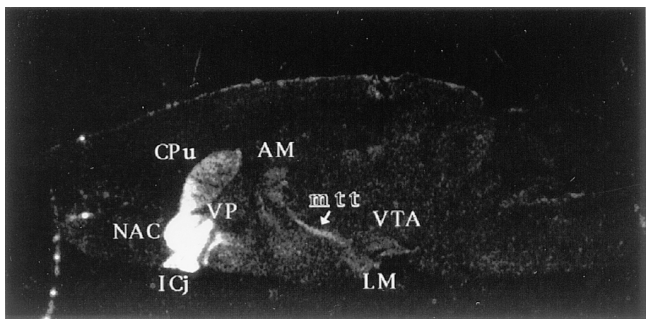


**Figure 6.** Darkfield photomicrograph of an autoradiogram of [$^{125}$I]PIPAT specific binding to $D_3$ sites in a rat sagittal section. Binding conditions were the same as described in Methods. Note labeling of the mtt. Image was overexposed to demonstrate binding in mtt. All abbreviations are as in Table 1.

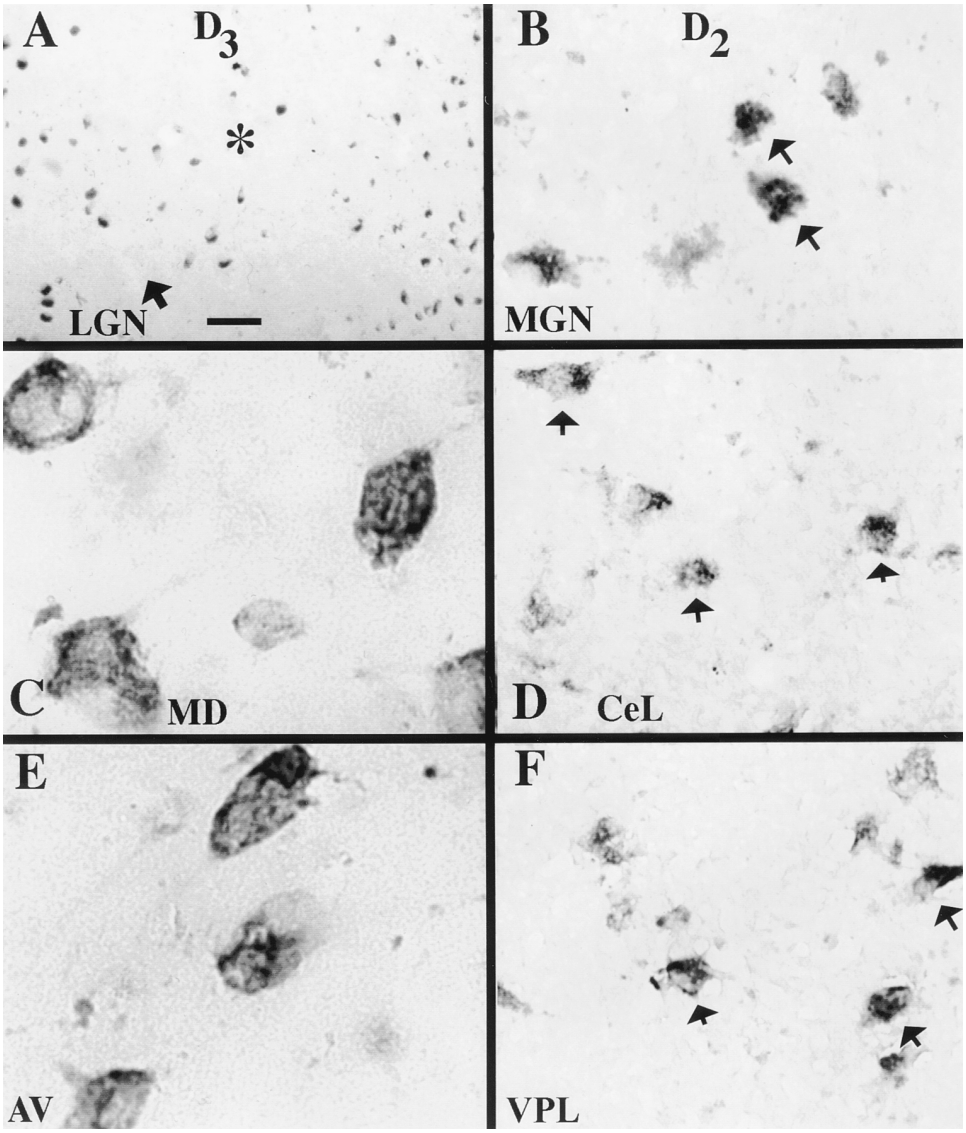


**Figure 7.** Neurons labeled with digoxigenin-labeled riboprobes for $D_3$ (left panel) and $D_2$ (right panel) receptor mRNA in the thalamus. A, $D_3$ mRNA positive cells in the LGN, arrow indicates deep magnocellular layer, asterisk = gap between the first and second layers; bar = 100 μm. B, $D_2$ mRNA positive neurons in the MGN; arrows show examples; bar = 20 μm. C, $D_3$ mRNA positive neurons in the MD; D, $D_2$ mRNA positive neurons in the CeL of the thalamus (arrows). E, $D_3$ mRNA positive neurons in the AV of the thalamus; bar = 10 μm. F, $D_2$ mRNA positive neurons in the ventral posterolateral nuclei of the thalamus (arrows indicate intensely labeled neurons); bar = 20 μm.

binding densities between various hypothalamic nuclei (Table 1; Figures 1A and C). In accordance with the distribution of $D_2$ receptor sites, neurons stained for $D_2$ mRNA were found in all major nuclei: periventricular, preoptic, dorsal, lateral, and posterior. The staining intensity varied from moderate to weak. The most intensely stained cells were observed in the lateral hypothalamic area and ventromedial nucleus. $D_3$ receptor sites were observed in all hypothalamic nuclei, but the densities were extremely low (Figures 1C and D; Figure 2). We were only able to consistently find neurons positive for $D_3$ mRNA in the MM (Figure 9A) and lateral hypothalamic area (data not shown). It is possible that $D_3$ positive cells also resided in other hypothalamic areas, because the receptor sites were present, but $D_3$ mRNA positive neurons in this region were extremely difficult to detect.

### Amygdala

As described previously (Joyce et al. 1991; Murray et al. 1994), $D_2$ receptor binding sites were found in most amygdaloid nuclei, but the amygdalostriatal transitional area (AStr) and the basolateral nucleus (BL) had considerably higher concentrations of the sites than any other area (Table 1 and Figure 5E). Within the BL higher concentrations of the $D_2$ sites were found in the intermediate, ventromedial, and dorsal subdivisions, while ventrolateral, and paralaminar subdivisions displayed lower concentrations. It should be noted, however, that binding densities in the basolateral nucleus varied considerably among individuals. In the central nucleus the concentration of $D_2$ binding sites was low, with islands of dense binding observed at the lateral border of the nucleus (Figure 5E; arrow). $D_2$ binding sites were present in the lateral nucleus in very low con-

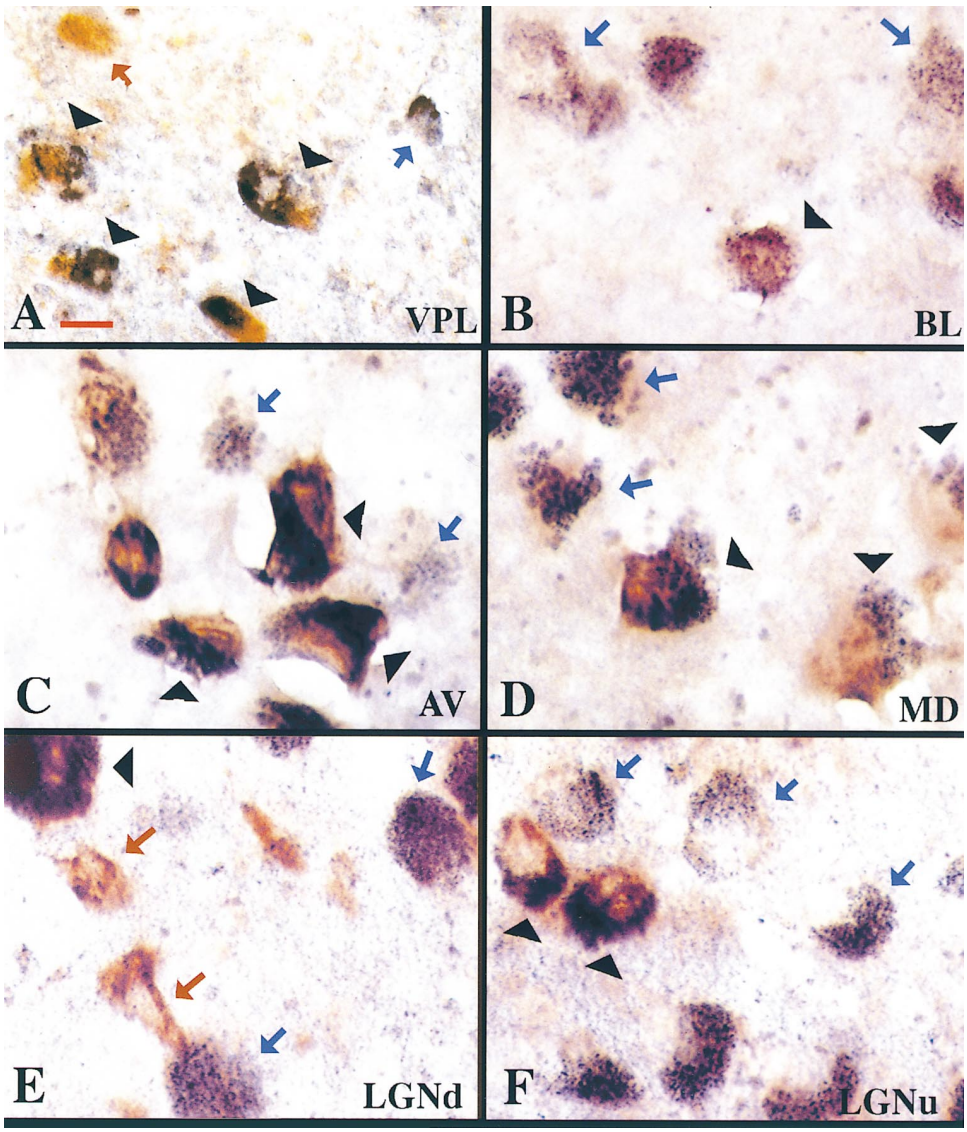


**Figure 8.** Neurons double labeled for $D_2$ and $D_3$ receptor mRNA. $D_2$ receptor mRNA was visualized as purple precipitate with granular appearance. $D_3$ receptor mRNA was visualized as bright brown precipitate with more homogenous appearance. In intensely double-labeled cells both colors partially overlap producing very dark almost black color. However, areas of brown and granular purple precipitate are distinguishable, most easily in the double-labeled cell with less intense signal. Rare cells labeled for $D_3$ mRNA only have bright homogenous brown color. A, lateral part of the ventral posterolateral nucleus of the thalamus; bar = 17 μm. B, dorsolateral subdivision of the BL of the amygdala; C, AV of the thalamus. D, medial part of the MD of the thalamus. E, deep layer. F, upper layer of the LGN. Bar for B-F = 8.7 μm. Black arrowheads indicate double-labeled cells; blue arrows = cells labeled solely for $D_2$ mRNA; and brown arrows = cells labeled solely for $D_3$ mRNA. All abbreviations are as in Table 1 except LGNd, deep layers of the LGN; and LGNu, upper layers of the LGN.

centration. Other amygdaloid nuclei had no detectable $D_2$ sites. $D_3$ receptor binding sites were observed in all amygdaloid nuclei (Table 1 and Figure 5F) in similar concentrations, except for the medial nucleus that had no detectable $D_3$ sites.

To a certain extent, the distribution of the $D_2$ and $D_3$ receptor sites was mirrored by the distribution of neurons expressing $D_2$ and $D_3$ mRNAs. The AStr displayed tightly packed darkly stained $D_2$ positive cells (Figure 9F). The most conspicuous mass of darkly stained $D_2$ mRNA positive large cells was observed in the dorsal part of BL (Figure 9D). Cells in the dorsolateral subdivision, as well as in medium-celled intermediate subdivision were also stained. Smaller neurons in the ventromedial and ventrolateral parts of the nucleus were often $D_2$ positive. $D_2$, but not $D_3$ mRNA positive neurons, were also found in the cell islands in the glomerular part of the paralaminar subdivision. A discrete belt of

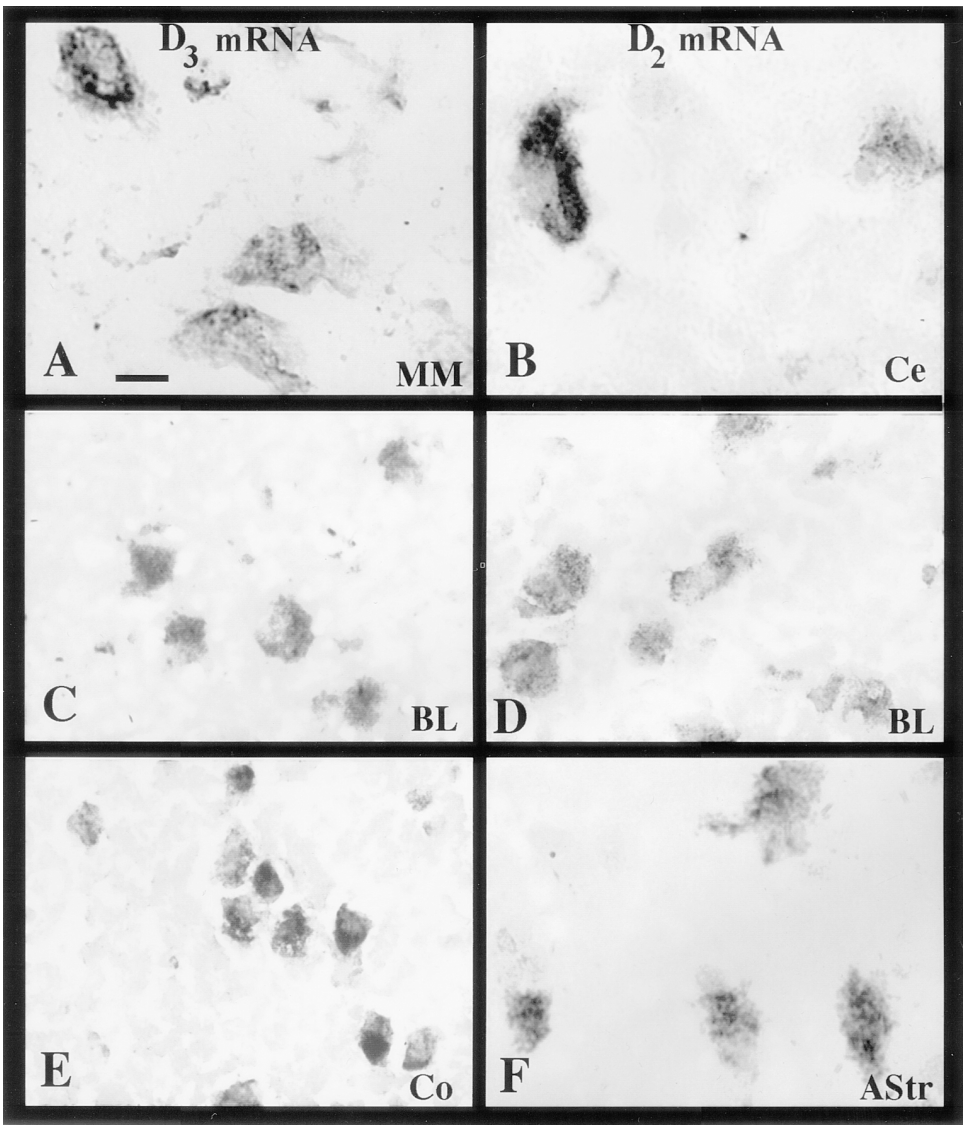


**Figure 9.** Neurons labeled for $D_2$ and $D_3$ receptor mRNA in the hypothalamus and amygdala. A, $D_3$ positive neurons in the MM. B, $D_2$ mRNA positive cells in the Ce of amygdala, positioned where the $D_2$ receptors are indicated by an arrow in Figure 5 E. C, $D_3$ mRNA positive neurons in the dorsolateral subdivision of the BL of the amygdala. D, $D_2$ mRNA positive neurons in the dorsal subdivision of the BL of amygdala. E, $D_3$ mRNA positive neurons in the Co of the amygdala. F, $D_2$ mRNA positive neurons in the AStr. Bar = 20 μm in C, D, E and 10 μm in A, B, F. All abbreviations are as in Table 1.

darkly stained $D_2$ positive neurons was observed in the lateral-most part of the lateral central nucleus, in the area of dense $D_2$ receptor binding. (Figure 9B). However, the distinction between frequency of $D_2$ positive cells or intensity of staining in the BL and the other amygdaloid nuclei was not nearly as striking as the difference in the concentrations of $D_2$ receptor binding sites. $D_2$ mRNA positive neurons were also observed in the lateral amygdaloid, cortical, and BM nuclei, where $D_2$ binding sites could not be consistently detected. Similarly to the arrangement of $D_2$ positive neurons, $D_3$ positive neurons were numerous in the dorso-lateral and dorsal parts of the BL (Figure 9C), which corresponded to the region of the highest density of $D_3$ binding sites (Figure 5F), but, in contrast with the $D_2$ mRNA positive cells, rarely detected in other subdivisons of the BL. $D_3$ as well $D_2$ mRNA positive neurons were observed in the cortical nucleus of the amygdala, especially in its dorsal subdivision (Figure 9E), as well as in the BM and, to a lesser extent, in the lateral nucleus. In spite of the presence of measurable concentrations of $D_3$ receptor sites in the amygdala, $D_3$ mRNA positive cells were relatively sparse, and staining intensity was generally low. However, neurons containing both mRNA species were identifiable, particularly in the BL (Figure 8B). Double labeled neurons accounted for 11.6 ± 5.6% of all labeled cells in the dorsal and dorsolateral subdivisions of BL, but were very rare in all other areas.

### Substantia Nigra and Ventral Tegmental Area

$D_2$ receptor sites were found in all groups of midbrain dopaminergic neurons (Table 1). Relatively high concentrations of receptor sites were observed in the ventral tegmental area (VTA) in the paranigral (PN) and parabrachial pigmented nuclei (PBP) (Figure 10C). Binding in the caudal linear nucleus (CLi) was also detectable. Conversely, few, if any, $D_3$ sites could be seen in the

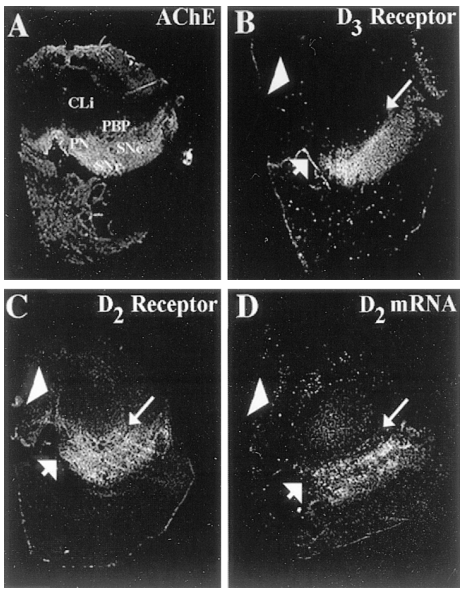


**Figure 10.** Darkfield photomicrographs of the tissue sections of the SN stained for AChE (A), labeled for $D_3$ receptors with [$^{125}$I]PIPAT (B), and for $D_2$ receptors with [$^{125}$I]epidepride (C) as described above, or for $D_2$ mRNA using $^{33}$P-labeled riboprobe (D). Large arrows indicate the position of the PBP; small arrows = the position of the PN; and arrowhead = the position of the CLi. Note the presence of $D_2$ receptors and mRNA both in the SN and VTA structures, including CLi, and the absence of $D_3$ binding sites in the PN and PBP. Also note dense $D_3$ binding in the SNr. All abbreviations are as in Table 1.

PN, PBP, or CLi (Figure 10B). $D_3$ receptor sites were detected throughout the substantia nigra pars reticulata (SNr), where $D_2$ sites were absent. The area of highest density of $D_3$ sites was located in the medial SNr. Thus, $D_2$ receptor binding was highest in the dorsal and ventral tiers of the substantia nigra pars compacta (SNc) but $D_3$ labeling was highest in the SNr (Figures 10B and C). Prevalence of $D_3$ rather than $D_2$ receptors in SNr is further illustrated in Figures 1A and B, which shows higher ratio of $D_3$ to $D_2$ binding sites in the rostral part of SNr.

The relative segregation of the $D_3$ from $D_2$ receptor subtype was not as clearly evident for the neurons expressing the respective mRNAs. $D_2$ receptor mRNA was detected in the large neuromelanin containing neurons of the SNc as well as in all components of the VTA using both isotopic (Figure 10D) and nonisotopic probes (Figures 11A–C). The PN (Figures 10D and 11A) as well as a considerable proportion of neurons in the PBP (Figures 10D and 11B) appeared heavily labeled for $D_2$ mRNA. The CLi, which is sparsely populated, displayed a number of $D_2$ mRNA-negative as well as $D_2$-positive cells (Figures 10D and 11C). Many neurons in the SN labeled for $D_2$ mRNA were TH-positive (Figure 11D). A few TH-negative cells that stained for $D_2$ mRNA were observed. $D_3$ mRNA was present in the large cells of the SNc, often co-localizing with $D_2$ mRNA (Figures 10B and 11E). Many neurons stained for $D_3$ mRNA were also TH-positive (Figure 11F). However, many cells were detected in SNc that contained $D_2$ but not $D_3$ mRNA. In the SNr, though, a number of predominantly small non-pigmented cells were single-labeled for $D_3$ mRNA. Only occasional $D_3$ mRNA positive cells were observed in the PBP and PN.

## DISCUSSION

The present study demonstrates the widespread distribution of both $D_2$ and $D_3$ receptor subtypes in the human brain. $D_2$ binding sites and $D_2$ mRNA positive neurons were widely distributed in the subcortical regions. As illustrated in Table 2 and Figure 12, the $D_3$ receptor was found in higher concentrations in a limited number of brain areas closely connected anatomically and functionally. In agreement with previous reports, we found that the $D_2$ receptors and mRNA were the most abundant in the dorsal CN and Pu (Joyce et al. 1991; Huntley et al. 1992; Murray et al. 1994; Meador-Woodruff et al. 1996), whereas $D_3$ receptor sites and mRNA were enriched in the ventral Pu and NAC, often in dense patches of binding and clusters of $D_3$ mRNA positive neurons, (Landwehrmeyer et al. 1993; Herroelen et al. 1994; Murray et al. 1994; Meador-Woodruff et al. 1996; Gurevich et al. 1997; Suzuki et al. 1998). NAC, which has the highest $D_3$ receptor concentration and number of $D_3$ mRNA positive neurons of all brain areas, projects primarily to the VP, medial part of the GPi and SNr (Haber et al. 1985; Lynd-Balta and Haber 1994a, 1994b), all regions enriched with the $D_3$ receptor and $D_3$ mRNA positive neurons. This is interesting, because cell morphology, connections, and neurochemical and physiological characteristics of the GPi and SNr are very similar (François et al. 1987; Yelnik et al. 1987). Though these two structures do not appear to be derived from the same developmental anlage (Marchand and Lajoie 1986; Marchand et al. 1986), they may be exposed to common developmental regulatory influences resulting in a higher level of expression of the $D_3$ receptor, which, in its turn, may contribute to unification of the structures, along with VP, into one functional system thus modulating the output of the limbic striatum. However, in the human brain, in contrast with the rat, distributions of $D_2$ and $D_3$ binding sites in the striatal areas were overlapping to a considerable degree suggesting that both subtypes mediate dopaminergic input in motor and limbic striatal areas. In pallidal and basal forebrain neurons both mRNA species were often detected, which may indicate functional importance of convergence of signals mediated by the two subtypes.

The thalamus and hypothalamus have not received much attention with regard to their dopaminergic in-

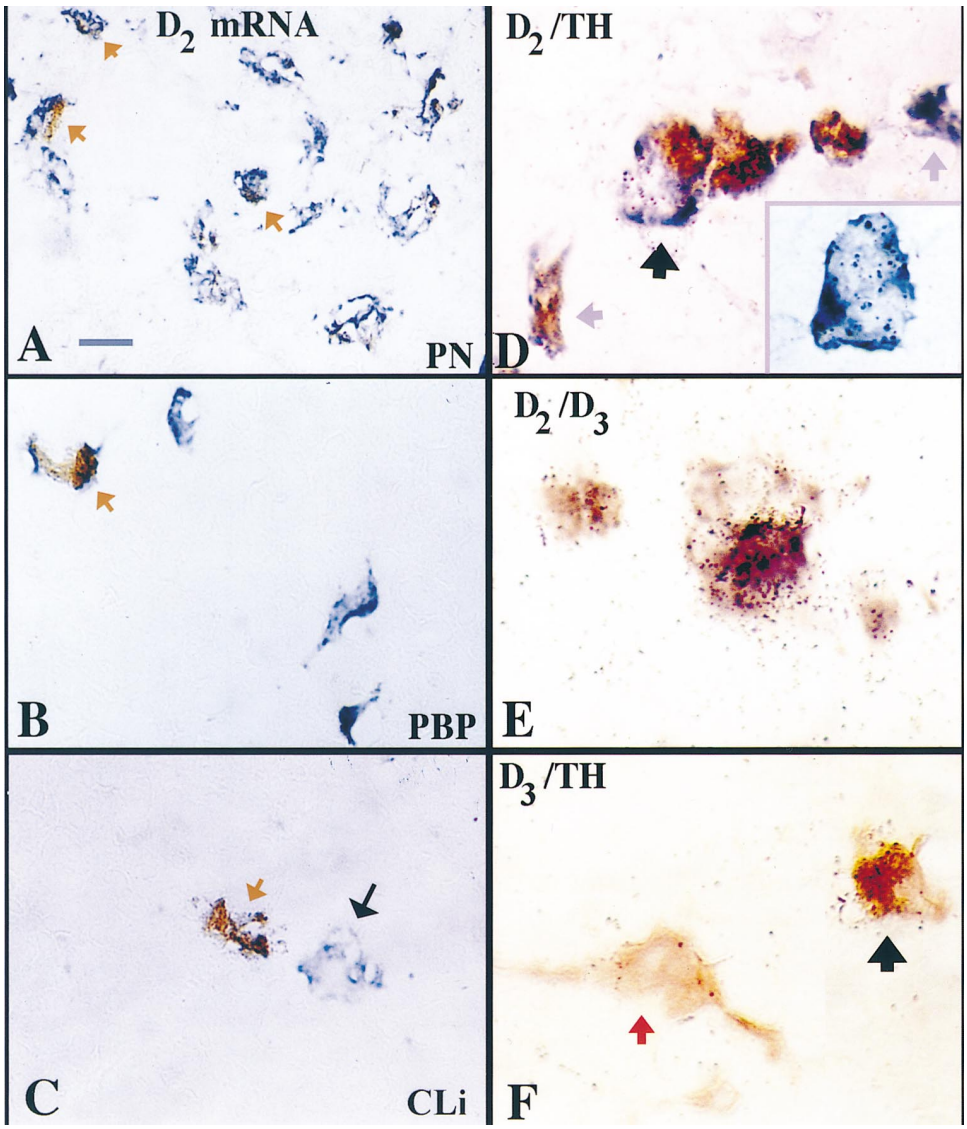


**Figure 11.** Neurons labeled for $D_2$ and $D_3$ mRNA in the SN and VTA. Left panel (A–C) shown neurons labeled solely for $D_2$ in the PN (A), PBP (B), and CLi (C) (×100; 1 cm = 0.02 mm). $D_2$ mRNA positive cells are blue colored. Melanized cells (brown color) are indicated by small brown arrows. Black arrow in C indicates non-melanized cell in the CLi stained blue for $D_2$ mRNA. D, colocalization of $D_2$ mRNA and TH immunoreactivity in neurons of the SNc. $D_2$ mRNA was visualized with $^{33}$P-labeled riboprobe, and the signal is represented by silver grains. TH immunoreactivity was visualized with SG peroxidase substrate (see Methods) that produces blue color. Brown color is neuromelanin found in many nigral cells. Large black arrow points at TH-positive melanin-containing cell also containing $D_2$ mRNA; insert shows a non-melanized TH-positive cell (blue color) containing $D_2$ receptor mRNA (silver grains); small purple arrow indicates melanized TH-positive cell that contains no $D_2$ receptor mRNA. E, colocalization of $D_2$ and $D_3$ mRNA in the SNc; $D_2$ mRNA was visualized with $^{33}$P-labeled riboprobe, and the signal is represented by silver grains above the cells. $D_3$ mRNA was visualized using digoxigenin-labeled riboprobe that is seen as purplish color. F, colocalization of $D_3$ mRNA and TH immunoreactivity (red color) in the SNc. $D_3$ mRNA is seen as silver grains above the cell, and TH immunoreactivity is seen as red color. Black arrows indicate double-labeled cells; red arrow = TH-positive cell negative for $D_3$ receptor mRNA. Bar represents in (A) 40 μm, in (B) and (C) 20 μm, and in (D–F) 10 μm. All abbreviations are as in Table 1.

nervation and expression of DA receptors, in part due to relatively low levels of all DA receptors. $D_2$ receptor sites in these regions were previously identified using membrane binding and autoradiography (Janowski et al. 1992; Kessler et al. 1993), and $D_2$ mRNA has been identified in the nonhuman primate (Choi et al. 1995). A recent report demonstrated the presence of D3 receptor mRNA in the human thalamus (Suzuki et al. 1998). Dopaminergic innervation to the rat LGB (Papadopoulus and Parnavelas 1990) and the human thalamus (Malais et al. 1990; Oke et al. 1992) has been demonstrated, though its sources are unknown. We have

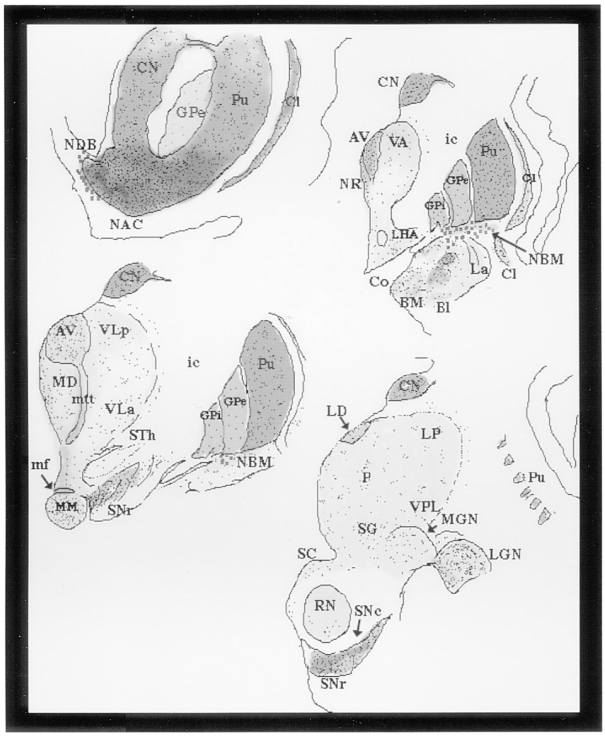


**Figure 12.** Schematic representation of the distribution of $D_3$ receptors and $D_3$ mRNA positive neurons in the subcortical areas of the human brain. Position and density of dots illustrate relative concentrations of $D_3$ mRNA positive cells. Large gray dots represent large neurons of the basal forebrain. Shades of gray represent relative densities of $D_3$ binding sites (darker shades correspond to higher concentrations of the sites). All abbreviations are as in Table 1.

shown $D_2$ and $D_3$ receptor sites and mRNA in many thalamic nuclei and throughout the hypothalamus of the human brain, though at considerably lower levels than in the striatum (Table 2 and Figure 12). In most thalamic areas the presence of $D_2$ or $D_3$ receptor sites coincided with the presence of their respective mRNA indicating that thalamic neurons are capable of synthesizing the receptor proteins. The most noticeable difference in distribution of $D_2$ and $D_3$ binding sites was the presence of a relatively high concentration of $D_2$ receptor sites in most intralaminar nuclei, which had little or no $D_3$ binding, and, in contrast, the presence of $D_3$ sites in the mtt, which contained no $D_2$ sites. The AV appears to represent a major site of interaction of the $D_2$ and $D_3$ receptors, because it possesses both types of binding sites in comparable concentrations as well as neurons expressing one or both mRNA species. The AV receives a nigrothalamic innervation from the SNr, a region of relatively higher expression of $D_3$ than $D_2$ receptors, via GABAergic nigrothalamic pathway (Ilinsky et al. 1985; Kultas-Ilinsky and Ilinsky 1990), which may be originating from non-dopaminergic $D_3$ mRNA positive neurons frequently observed in SNr. The AV also receives massive projections from the MM through the mtt, the former enriched with $D_3$ mRNA and the latter with binding sites. Although functions of the AV remain little understood, it has been implicated in mechanisms of memory and attention (von Cramon et al. 1985). Its connections with the prefrontal, temporal, cingulate, and entorhinal cortex and hippocampal formation (for review see Armstrong 1990) suggest its importance for processing of information within the limbic circuit. Relative enlargement of the human AV comparing to other antropoids (Armstrong 1986) implies its involvement in specific complex aspects of behavior. Among sensory thalamic nuclei, the LGB, and to a lesser degree, the MGB possess $D_2$ and $D_3$ receptor binding sites and both mRNA species. Recent data have indicated the presence of dopaminergic fibers (Papadopoulus and Parnavelas 1990) and DA receptors (Bouthenet et al. 1987; Huang et al. 1992) in the rat LGB, and $D_3$ receptor mRNA in the human LGB (Suzuki et al. 1998). In the rat, neurons of the LGB respond to application of $D_2$ agonists by increased baseline activity, an effect that was reversible by specific $D_2$ antagonists (Albrecht et al. 1996). In both nuclei $D_3$ and $D_2$ mRNA co-localize to a considerable proportion of neurons in magnocellular laminae 1 and 2, whereas in upper laminae $D_2$ mRNA positive neurons predominate. Principal auditory, visual, and somatosensory information to the cortex passes through the ventral posterior and geniculate nuclei. Complex association pathways involve orbitofrontal and dorsolateral prefrontal cortices and their projections from the anterior and medial nuclei of the thalamus (Groenewegen et al. 1990). Investigators have proposed that in schizophrenia there are disturbances in the filtering of sensory signals in these thalamo-cortical pathways (Carlsson and Carlsson 1990). These data suggest the modulatory role of the dopaminergic system and $D_2$-like receptors not only in the limbic but also sensory thalamic nuclei, which may be particularly important for pathophysiology of schizophrenia and regulation of psychotic symptoms by DA antagonists.

We had previously described the presence of $D_2$ and $D_3$ receptor sites in the basal forebrain and amygdala (Murray et al. 1994). Concentration of $D_2$ receptors and mRNA exceeds that of $D_3$ receptor in both NBM and NDB. The predominant phenotype of neurons expressing either mRNA species appears to be cholinergic, and many of them co-express $D_2$ and $D_3$ mRNAs. The $D_3$ receptor was present in all amygdaloid nuclei at low levels and was more abundant in the magnocellular dorsolateral and dorsal subdivisions of the BL. The $D_2$ receptor was particularly abundant in the AStr and BL comparing to all other amygdaloid areas. Some of the large neurons of the dorso-lateral BL co-expressed $D_2$ and $D_3$ mRNA. The cholinergic neurons of the NBM and NDB and the amygdaloid nuclei, particularly the central, basal, and lateral nuclei, are provided with

dopaminergic innervation from the VTA and medial components of the SN (Sadikot and Parent 1990; Takada 1990; Gaykema and Zaborszky 1996; Zaborszky and Cullianan 1996). This may be important in some of the cognitive difficulties associated with damage to the mesolimbic DA system in Parkinson disease (Torack and Morris 1988), perhaps through modulation of the cholinergic system innervating the cortex (Zaborszky et al. 1993). The amygdala has long been recognized as playing a role in emotional and affective experiences (Aggleton 1992). The amygdala sends extensive input to the ventral striatum (Zahm and Brog 1992; Kunishio and Haber 1994) providing additional limbic input that may be under control of DA via $D_2$ and $D_3$ receptors. Hence, it may be of value to consider $D_2$ receptors in BL and AStr and $D_3$ receptors in BL as important targets for antipsychotics. The regions of the amygdala expressing the highest levels of $D_2$ and $D_3$ receptors exhibit profound reductions of $D_2$-like receptors in Alzheimer disease (Joyce et al. 1993) suggesting a region-specific dopaminergic vulnerability that may underlie some of the affective disturbances accompanying cognitive impairment in this disorder (Bungener et al. 1996; Cadieux and Greve 1997).

Dopamine $D_2$ and $D_3$ receptors are believed to be expressed in dopaminergic neurons of the midbrain (Bouthenet et al. 1991; Diaz et al. 1995; Meador-Woodruff et al. 1994a), where they are thought to act as autoreceptors (Rivet et al. 1994; Nissbrandt et al. 1995). Our data demonstrating both $D_2$ receptor sites and mRNA in TH-positive neurons of the SNc and SNr are consistent with these findings. The $D_3$ receptor predominates in the rostral SNr, whereas in the SNc the $D_2$ receptor concentration exceeds that of the $D_3$ receptors. One particularly important difference with the rat is that $D_3$ receptors are virtually absent in the PN, CLi, and PBP that together comprise the VTA. This contrasts with studies in the rat where $D_3$ mRNA is evident in the VTA, SNr and pars lateralis (Diaz et al. 1995). Although $D_2$ mRNA is reported to be present in the rat VTA, one report for the human has indicated a virtual absence there of $D_2$ mRNA expressing cells (Meador-Woodruff et al. 1994a). However, in the present study we found both $D_2$ receptor sites and mRNA in all dopaminergic cell groups of the midbrain, including the VTA. Hurd et al. (1994) have also observed $D_2$ receptor mRNA in the VTA, but at levels significantly lower than the SN. The reason for this discrepancy between the results of Meador-Woodruff and associates (1994a) and our work is unclear. The concentration of $D_2$ receptor sites and mRNA expression in the CLi in our material was not high, and we observed many $D_2$ negative cells. Nonetheless, $D_2$ receptor sites and mRNA were clearly detected in the VTA, especially in the PN, as well as in SN. We conclude that, similarly to the rat brain, in the human brain the $D_2$ (but probably not $D_3$) receptor plays an autoreceptor role in both dopaminergic cell groups.

The present study demonstrates that in the human brain many $D_3$ mRNA positive neurons also express $D_2$ mRNA. The combined evidence of the mRNAs' co-expression and overlap in the distribution of the receptor sites suggests that in many areas a considerable proportion of neurons co-express functional $D_2$ and $D_3$ receptors. This proportion varies among areas depending largely on the concentration of the more rare $D_3$ mRNA. In the areas rich in $D_3$ receptors and mRNA, cells double-labeled for $D_2$ and $D_3$ mRNA predominate, with only occasional single-labeled $D_3$ mRNA positive neurons. Such areas include the basal forebrain, LGN, medial part of the AV and MD of the thalamus, SNc and SNr. By contrast, in the majority of brain areas $D_2$ mRNA positive neurons far outnumber $D_3$ mRNA positive neurons, and single-labeled $D_2$ mRNA positive neurons are frequently observed. Several technical considerations, however, are important for the interpretation of these results. In our double-labeling experiments positive detection of both mRNA species was emphasized. Detection of both species is obviously facilitated when both mRNAs are present at similar levels. In cells that contain one mRNA in considerably higher concentration than the other the low-abundance mRNA may not be observed. This is particularly a problem for $D_3$ receptor mRNA because it is usually present at low levels compared to $D_2$ mRNA. Thus, some neurons that have been identified as solely expressing $D_2$ mRNa may have also expressed $D_3$ mRNA in concentrations near or below our level of detection. In view of these constraints, positive double-labeling of $D_2$ and $D_3$ mRNA in the same cells may be viewed with a fairly high degree of confidence, but the failure to observe double-labeling should be interpreted with caution. In addition, the method of double-ISHH used in this study is sensitive to cell size, shape, call density, and subcellular mRNA localization. It is particularly suitable for large cells or cells where the two mRNAs are spatially segregated subcellularly. In some brain areas comprised of relatively small cells such as Pu, CN, NAC, the labels were impossible to detect reliably in the same cell because they masked each other. The conclusions we can most reliably draw are, therefore, that 1) in most regions in the forebrain $D_2$ receptor mRNA is present at much higher levels than $D_3$ receptor mRNA; 2) in a few regions of the forebrain $D_3$ receptor mRNA predominates; and 3) $D_2$ and $D_3$ receptor mRNA are often co-expressed in cells, particularly in areas where $D_3$ mRNA expression is abundant.

## CONCLUSION

Based on studies in the rat, Sokoloff and associates (Sokoloff et al. 1990; Sokoloff and Schwartz 1995) have

made the valuable suggestion that the $D_3$ receptor is a particularly important target for antipsychotics in the mesolimbic DA system. The present study in the human demonstrates that the distribution of $D_3$ receptors and $D_3$ mRNA-bearing neurons is consistent with relative segregation of the $D_3$ subtype to the limbic striatum as well as it primary and secondary targets and many sources of its afferents. The nucleus accumbens and adjacent ventral putamen, referred to as the ventral or limbic striatum, exhibit the highest expression of $D_3$ receptor binding sites and corresponding levels of $D_3$ mRNA. These regions are the targets of the mesolimbic DA system receiving input from the medial and dorsal components of the SN (Jimenez-Castellanos and Graybiel 1987; Lynd-Balta and Haber 1994a; Haber and Fudge 1997). Additional sources of input to the limbic striatum include regions enriched in $D_3$ receptors such as the anterior nuclei of the thalamus and NBM. The ventral striatum projects primarily to the VP, the most medial part of the GPi and SNr (Haber et al. 1985; 1994; Lynd-Balta and Haber 1994a), which are also enriched with $D_3$ receptors and $D_3$ mRNA positive neurons. These regions provide input to the anterior nuclei of the thalamus (Groenewegen et al. 1990). The AV of the thalamus, which exhibits the highest expression of $D_3$ receptors within the thalamus, receives a nigrothalamic GABAergic innervation from the SNr (Ilinsky et al. 1985), a region of relatively higher expression of $D_3$ and $D_2$ receptors. This provides multiple sites at which drugs such as antipsychotics might act to regulate activity in the "limbic" loop via interaction with the $D_3$ receptor. However, in contrast with the rat, in the human brain the $D_3$ receptor is also expressed at high levels in the motor striatum. Other brain regions thought to be involved in sensory (sensory thalamic nuclei), hormonal (mmt) and association (amygdala) functions also express the $D_3$ receptor, often co-expressed with the $D_2$ receptor.

The extensive co-localization of $D_2$ and $D_3$ receptors in human forebrain raises a question about the functional significance of the simultaneous presence of pharmacologically similar DA receptors in the same cell. As has been proposed (Diaz et al. 1995; Sokoloff and Schwartz 1995), the significantly higher affinity of the $D_3$ receptor for DA may enable it to serve in vivo as an extrasynaptic receptor responding to low concentrations of DA at distances remote from the point of DA release. Conversely, the $D_2$ receptor with its low affinity to DA is likely to respond to high synaptic concentrations of DA. Thus, brain areas with relatively high densities of $D_3$ receptors may be under tonic regulatory influence of the brain dopaminergic system, even if the dopaminergic innervation is sparse. $D_2$ and $D_3$ receptors may elicit opposing responses in neurons (Diaz et al. 1995; Lévesque et al. 1995; Surmeier et al. 1996), and may respond differently to loss of DA (Lévesque et al. 1995) or antipsychotic treatment (reviewed in Joyce and Meador-Woodruff 1997). Our data provide initial insight into details of distribution and co-expression of DA $D_2$ and $D_3$ receptors in the human brain. Intricate interplay of signaling by related but not identical DA receptors in different brain areas and individual neurons remains to be elucidated. Perhaps, circuits with high $D_3$ receptor expression and other functionally connected systems with predominance of the $D_2$ receptor provide different target systems for DA antagonists in regulation of psychotic symptoms.

## ACKNOWLEDGMENTS

This research was supported by an award from Scottish Rite Benevolent Foundation's Schizophrenia Research Program, N.M.J., U.S.A., and by U.S. Public Health Service Grants MH 56824, and AG 09215. We thank Lucia Sue for providing some of the specimens used in this study. We also thank Drs. Joseph Rogers and Wendy Thomas for critical reading of the manuscript and helpful comments.

## REFERENCES

Aggleton JP (1992): The functional effects of amygdala lesions in humans: A comparison with findings from monkeys. In Aggleton JP (ed), The Amygdala: Neurobiological Aspects of Emotion, Memory, and Mental Dysfunction. New York, NY, Wiley-Liss, pp 485–503

Albrecht D, Quäschling U, Zippel U, Davidowa H (1996): Effects of dopamine on neurons of the LGN: An ionophoretic study. Synapse 23:70–78

Alheid GF, Heimer L, Switzer III RC (1990): Basal ganglia. In Paxinos G (ed), The Human Nervous System. San Diego, Academic Press, pp 483–583

Armstrong E (1986): Enlarged limbic structures in the human brain: The anterior thalamus and medial mamillary body. Brain Res 362:394–397

Armstrong E (1990): Limbic thalamus: Anterior and mediodorsal nuclei. In Paxinos G (ed), The Human Nervous System. San Diego, Academic Press, pp 469–483

Bouthenet M-L, Martres MP, Sales N, Schwartz JC (1987): A detailed mapping of dopamine D2 receptors in rat central nervous system by autoradiography with [$^{125}$I]iodosulpride. Neuroscience 20:117–155

Bouthenet M-L, Souil E, Martres M-P, Sokoloff P, Giros B, Schwartz J-C (1991): Localization of dopamine D3 receptor mRNA in the rat brain using in situ hybridization histochemistry: Comparison with dopamine D2 receptor mRNA. Brain Res 564:203–219

Bungener C, Jouvent R, Derouesne C (1996): Affective disturbances in Alzheimer's disease. J Am Geriatr Soc 44:1066–1071

Cadieux NL, Greve KW (1997): Emotion processing in Alzheimer's disease. J Int Neuropsychol 3:411–419

Caine SB, Koob GF (1993): Modulation of cocaine self-administration in the rat through D3 dopamine receptors. Science 260:1814–1816

Carlsson M, Carlsson A (1990): Schizophrenia: a subcortical neurotransmitter imbalance syndrome. Schizophr Bull 16:425–432

Choi WS, Machida CA, Ronnekleiv OK (1995): Distribution of dopamine D1, D2, and D5 receptor mRNAs in the monkey brain: Ribonuclease protection assay analysis. Mol Brain Res 31:86–94

Diaz J, Lévesque D, Lammers CH, Griffon N, Martres M-P, Schwartz J-C, Sokoloff P (1995): Phenotypical characterization of neurons expressing the dopamine D3 receptor in the rat brain. Neuroscience 65:731–745

François C, Yelnik J, Percheron G (1987): Golgi study of the primate substantia nigra. II. Spatial organization of dendritic arborization in relation to the cytoarchitectonic boundaries and to the striatonigral bundle. J Comp Neurol 265:473–493

Gaykema RP, Zaborszky L (1996): Direct catecholaminergic-cholinergic interaction in the basal forebrain. II. Substantia nigra-ventral tegmental area projection to cholinergic neurons. J Comp Neurol 374:555–577

Groenewegen HJ, Berendse HW, Wolters JG, Lohman AH (1990): The anatomical relationship of the prefrontal cortex with the striatopallidal system, the thalamus and the amygdala: Evidence for a parallel organization. Prog Brain Res 85:95–116

Gurevich EV, Joyce JN (1996): Distribution of dopamine (DA) D3 receptor mRNA and D2 receptor mRNA in the human forebrain. Soc Neurosci Abstr 22:1581

Gurevich EV, Bordelon Y, Shapiro RM, Arnold SE, Gur RE, Joyce JN (1997): Mesolimbic dopamine D3 receptors and use of antipsychotics in patients with schizophrenia: A postmortem study. Arch General Psychiatry 54:225–232

Haber SN, Groenewegen HJ, Grove EA, Nauta WJ (1985): Efferent connections of the ventral pallidum: evidence of a dual striato pallidofugal pathway. J Comp Neurol 235:322–335

Haber SN, Groenewegen JH (1989): Interrelationship of the distribution of neuropeptides and tyrosine hydroxylase immunoreactivity in the human substantia nigra. J Comp Neurol 290:53–68

Haber SN, Lynd-Balta E, Spooren WPJM (1994): Integrative aspects of basal ganglia circuitry. Adv Beh Biol 41:71–80

Haber SN, Fudge JL (1997): The primate substantia nigra and VTA: Integrative circuitry and function. Critical Rev Neurobiol 11:323–342

Heckers S, Geula C, Mesulam M-M (1992): Cholinergic innervation of the human thalamus: Dual origin and differential nuclear distribution. J Comp Neurol 325:68–82

Herroelen L, De Backer J-P, Wilczak N, Flamez A, Vanquelin G, De Keyser J (1994): Autoradiographic distribution of D3-type dopamine receptors in human brain using [$^3$H] 7-hydroxy-N,N-di-n-propyl-2-aminotetralin. Brain Res 648:222–228

Huang Q, Zhou D, Chase K, Gusella JF, Aronin N, DiFiglia M (1992): Immunohistochemical localization of the D1 dopamine receptor in rat brain reveals its axonal transport, pre- and postsynaptic localization, and prevalence in the basal ganglia, limbic system, and thalamic reticular nucleus. Proc Nat Acad Sci 89:11988–11992

Huntley GW, Morrison JH, Prikhozhan A, Sealfon SC (1992): Localization of multiple dopamine receptor subtype mRNA in human and monkey motor cortex and striatum. Mol Brain Res 15:181–188

Hurd YL, Pristupa ZB, Herman MM, Niznik HB, Kleinman JE (1994): The dopamine transporter and dopamine D2 receptor messenger RNAs are differentially expressed in limbic- and motor-related subpopulations of human mesencephalic neurons. Neuroscience 63:357–362

Ilinsky IA, Jouandet MR, Goldman-Rakic PS (1985): Organization of the nigrothalamocortical system in the rhesus monkey. J Comp Neurol 236:315–330

Janowski A, Neve KA, Kinzie JM, Taylor B, de Paulis T, Belkmar JK (1992): Extrastriatal dopamine D2 receptors: Distribution, pharmacological characterization and region-specific regulation by clozapine. J Pharmacol Exp Ther 261:1282–1290

Jimenez-Castellanos J, Graybiel AM (1987): Subdivisions of the dopamine-containing A8-A9-A10 complex identified by their differential mesostriatal innervation of striosomes and extrastriosomal matrix. Neuroscience 23:223–242

Jones EG (1990): Correlation and revised nomenclature of ventral nuclei in the thalamus of human and monkey. Stereotact Funct Neurosurg 54, 55:1–20

Joyce JN, Sapp DW, Marshall JF (1986): Human striatal dopamine receptors were organized in patches. Proc Natl Acad Sci USA 83:8002–8006

Joyce JN, Janowski A, Neve KA (1991): Characterization and distribution of [$^{125}$I]Epidepride binding to dopamine D2 receptors in basal ganglia and cortex of human brain. J Pharmacol Exp Ther 253:1253–1263

Joyce JN, Kaeger C, Ryoo H, Goldsmith S (1993): Dopamine D2 receptors in the hippocampus and amygdala in Alzheimer's disease. Neurosci Lett 154:171–174

Joyce JN, Meador-Woodruff JH (1997): Linking the family of D2 receptors to neuronal circuits in human brain: Insights into schizophrenia. Neuropsychopharmacology 16:375–384

Kessler RM, Whetsell WO, Sib Ansari M, Votaw JR, de Paulis T, Clanton JA, Schmidt DE, Mason S, Manning RG (1993): Identification of extrastriatal dopamine D2 receptors in postmortem human brain with [$^{125}$I] epidepride. Brain Res 609:237–243

Kultas-Ilinsky K, Ilinsky IA (1990): Fine structure of the magnocellular subdivision of the ventral anterior thalamic nucleus (Vamc) of Macaca mulatta: II. Organization of nigrothalamic afferents as revealed with EM autoradiography. J Comp Neurol 294:479–489

Kunishio K, Haber SN (1994): The primate striatal projections from the amygdala and hippocampus: A retrograde study. Soc Neurosci Abstr 20:333

Landwehrmeyer B, Mengold G, Palacios JM (1993): Dopamine D3 receptor mRNA and binding sites in human brain. Mol Brain Res 18:187–192

Le Moine C, Bloch B (1996): Expression of the D3 dopamine receptor in peptidergic neurons of the nucleus accumbens: comparison with the $D_1$ and D2 dopamine receptors. Neuroscience 73:131–143

Lévesque D, Martres M-P, Diaz J, Griffon N, Lammers CH, Sokoloff P, Schwartz J-C (1995): A paradoxical regula-

tion of the dopamine D3 receptor expression suggests the involvement of an anterograde factor from dopamine neurons. Proc Natl Acad Sci USA 92:1719–1723

Lynd-Balta E, Haber SN (1994a): The organization of midbrain projections to the ventral striatum in the primate. Neuroscience 59:609–623

Lynd-Balta E, Haber SN (1994b): Primate striatonigral projections: A comparison of the sensorimotor-related striatum and the ventral striatum. J Comp Neurol 345:562–578

Malais P, Waltregny A, Maula A, Dresse A (1990): Dopamine and acetylcholine release in thalamus of non-parkinsonian and parkinsonian subjects. Acta Neurol Belg 90: 200–206

Marchand R, Lajoie L (1986): Histogenesis of the striopallidal system in the rat. Neuroscience 17:573–590

Marchand R, Lajoie L, Lanchet C (1986): Histogenesis at the level of the basal forebrain: The entopeduncular nucleus. Neuroscience 17:591–607

Meador-Woodruff JH, Mansour A, Healy DJ, Kuehn R, Zhou QY, Bunzow JR, Akil H, Civelli O, Watson SJ Jr (1991): Comparison of the distributions of D1 and D2 dopamine receptor mRNAs in rat brain. Neuropsychopharmacology 5:231–242

Meador-Woodruff JH, Damask SP, Watson SJ (1994a): Differential expression of autoreceptors in the ascending dopamine systems of the human brain. Proc Nat Acad Sci USA 91:8297–8301

Meador-Woodruff JH, Grandy DK, Van Tol HHM, Damask SP, Little KY, Civelli O, Watson SJ (1994b): Dopamine receptor gene expression in the human medial temporal lobe. Neuropsychopharmacology 10:239–248

Meador-Woodruff JH, Damask SP, Wang J, Haroutunian V, Davis KL, Watson SJ (1996): Dopamine receptor mRNA expression in human striatum and neocortex. Neuropsychopharmacology 15:17–29

Murray AM, Ryoo H, Gurevich EV, Joyce JN (1994): Localization of dopamine D3 receptors to mesolimbic and D2 receptors to mesostriatal regions of human forebrain. Proc Nat Acad Sci USA 91:11271–11275

Nissbrandt H, Ekman A, Eriksson E, Heilig M (1995): Dopamine D3 receptor antisense influences dopamine synthesis in rat brain. NeuroReport 6:573–576

Ohye C (1990): Thalamus. In Paxinos G (ed), The Human Nervous System. San Diego, Academic Press, pp 439–469

Oke AF, Putz C, Adams RN, Bird ED (1992): Neuroleptic treatment was an unlikely cause of elevated dopamine in thalamus of schizophrenic subjects. Psychiatry Res 45:203–208

de Olmos J (1990): Amygdaloid nuclei gray complex. In Paxinos G. (ed), The Human Nervous System. San Diego, Academic Press, pp 583–711

Papadopoulus GC, Parnavelas JG (1990): Distribution and synaptic organization of dopaminergic axons in the lateral geniculate nucleus of the rat. J Comp Neurol 294:356–361

Paxinos G, Tork I, Halliday G, Mehler W (1990): Human homologs to brainstem nuclei identified in other animals as revealed by acetylcholinesterase activity. In Paxinos G (ed), The Human Nervous System. San Diego, Academic Press, pp 149–203

Rivet J-M, Audinot V, Gobert A, Peglion J-L, Millan MJ (1994): Modulation of mesolimbic dopamine release by the selective dopamine D3 receptor antagonist, (+) -S 14297. Eur J Pharmacol 265:175–177

Sadikot AF, Parent A (1990): The monoaminergic innervation of the amygdala in the squirrel monkey: An immunohistochemical study. Neuroscience 36:431–447

Saper CB (1990): Hypothalamus. In Paxinos G (ed), The Human Nervous System. San Diego Academic Press, pp 389–415

Sibley DR, Monsma FJ, Shen Y (1993): Molecular neurobiology of D1 and D2 dopamine receptors. In Waddington JL (ed), Neuroscience and Psychopharmacology: D1:D2 Dopamine Receptor Interactions. San Diego, Academic Press, pp 1–21

Sims KS, Williams RS (1990): The human amygdaloid complex: A cytologic and histochemical atlas using Nissl, acetylcholinesterase and nicotinamid adenine dinucleotide phosphate diaphorase staining. Neuroscience 36: 449–472

Sokoloff P, Giros B, Martres MP, Bouthenet ML, Schwartz JC (1990): Molecular cloning and characterization of a novel dopamine receptor (D3) as a target for neuroleptics. Nature 347:146–151

Sokoloff P, Schwartz J-C (1995): Novel dopamine receptors half a decade later. TIPS 16:270–275

Staley JK, Mash DC (1996): Adaptive increase in D3 dopamine receptors in the brain reward circuits of human cocaine fatalities. J Neurosci 16:6100–6106

Surmeier DJ, Wen-Jie S, Zhen Y (1996): Coordinated expression of dopamine receptors in neostriatal medium spiny neurons. J Neurosci 16:6579–6591

Suzuki M, Hurd YL, Sokoloff P, Schwartz J-C, Sedvall G (1998): D3 dopamine receptor mRNA is widely expressed in the human brain. Brain Res 779:58–74

Takada M (1990): The A11 catecholamine cell group: another origin of the dopaminergic innervation of the amygdala. Neurosci Lett 118:132–135

Torack RM, Morris JC (1988): The association of ventral tegmental area histopathology with adult dementia. Arch Neurol 45:497–501

von Cramon DY, Hebel N, Schuri U (1985): A contribution to the anatomical basis of thalamic amnesia. Brain 108:993–1008

Yelnik J, François C, Percheron G, Heyner S (1987): Golgi study of the primate substantia nigra. I. Quantitative morphology and typology of nigral neurons. J Comp Neurol 265:455–472

Zaborszky L, Cullianan WE (1996): Direct catecholaminergic-cholinergic interactions in the basal forebrain. I. Dopamine-beta-hydroxylase- and tyrosine hydroxylase input to cholinergic neurons. J Comp Neurol 374:534–554

Zaborszky L, Cullinan WE, Luiine VN (1993): Catecholaminergic-cholinergic interaction in the basal forebrain. Prog Brain Res 98:31–49

Zahm DS, Brog JS (1992): On the significance of subterritories in the "accumbens" part of the ventral striatum. Neuroscience 50:751–767